Hepatic Gluconeogenesis Is Enhanced by Phosphatidic Acid Which Remains Uninhibited by Insulin in Lipodystrophic Agpat2−/− Mice*

Shireesha Sankella‡, Abhimanyu Garg‡, Jay D. Horton§¶‖, and Anil K. Agarwal‡1

From the ‡Division of Nutrition and Metabolic Diseases, Department of Internal Medicine and Center for Human Nutrition, §Division of Digestive and Liver Diseases and Departments of ¶Molecular Genetics and ‖Biochemistry, University of Texas Southwestern Medical Center, Dallas, Texas 75390

Background: Lipodystrophic Agpat2−/− mice are severely diabetic and insulin resistant.
Results: Livers of Agpat2−/− mice have elevated levels of phosphatidic acids (PAs), which enhance gluconeogenesis.
Conclusion: PA enhanced hepatic gluconeogenesis contributes to the hyperglycemia present in Agpat2−/− mice.
Significance: PA enhanced hepatic gluconeogenesis might have wider implications in understanding the development of hyperglycemia in type 2 diabetes.

In this study we examined the role of phosphatidic acid (PA) in hepatic glucose production (HGP) and development of hepatic insulin resistance in mice that lack 1-acylglycerol-3-phosphate O-acyltransferase 2 (AGPAT2). Liver lysophosphatidic acid and PA levels were increased ∼2- and ∼5-fold, respectively, in male Agpat2−/− mice compared with wild type mice. In the absence of AGPAT2, the liver can synthesize PAs by activating diacylglycerol kinase or phospholipase D, both of which were elevated in the livers of Agpat2−/− mice. We found that PAs C16:0/18:1 and C18:1/20:4 enhanced HGP in primary WT hepatocytes, an effect that was further enhanced in primary hepatocytes from Agpat2−/− mice. Lysophosphatidic acids C16:0 and C18:1 failed to increase HGP in primary hepatocytes. The activation of HGP was accompanied by an up-regulation of the key gluconeogenic enzymes glucose-6-phosphatase and phosphoenolpyruvate carboxykinase. This activation was suppressed by insulin in the WT primary hepatocytes but not in the Agpat2−/− primary hepatocytes. Thus, the lack of normal insulin signaling in Agpat2−/− livers allows unrestricted PA-induced gluconeogenesis significantly contributing to the development of hyperglycemia in these mice.

White adipose tissue is a key organ involved in glucose and lipid homeostasis. White adipose tissue stores excess fatty acids as triacylglycerol and releases free fatty acids via lipolysis. The 1-acyl-glycerol-3-phosphate O-acyltransferase (AGPAT)[2] enzymes con-vert 1-acylglycerol-3-phosphate (lysophosphatidic acid, LPA) to 1,2-diacylglycerol-3-phosphate (phosphatidic acid, PA) and play a critical role in the biosynthesis of triacylglycerols and glycerophospholipids (1, 2).

There are at least 11 known isoforms of AGPAT, each encoded by a different gene (3). We have previously reported that AGPAT2 mutations result in autosomal recessive congenital generalized lipodystrophy type 1 (CGL1) (4). Patients with CGL1 are born without any detectable white adipose tissue but still develop severe insulin resistance (IR) and type 2 diabetes in their first decade of life and, in some, the IR is so severe that it manifests as acanthosis nigricans, hypertriglyceridemia, hepatic steatosis, and type 2 diabetes (5, 6).

To further understand the physiological role of AGPAT2 in the pathogenesis of lipodystrophy associated metabolic complications, we developed and phenotyped an Agpat2 knock-out mouse (7). These mice lack both brown adipose and white adipose tissue and recapitulate all of the features manifest in human CGL1. The livers of Agpat2−/− mice have ∼10% residual AGPAT activity compared with wild type (WT) mice. The marked reduction in AGPAT activity would predict significantly lower hepatic PA levels. Surprisingly, total glycerophospholipid levels in the livers of Agpat2−/− mice were not very different from those of WT mice (7). Similar observations were reported in cultured OP9 cells, a cultured cell model for adipogenesis (8). Inhibiting Agpat2 expression in these cells using siRNA indicated that additional pathway(s) might exist to generate PA (8).

Here, we used Agpat2−/− mice to determine whether PAs contribute to the development of IR in liver. PA can bind to the FK506-binding protein (FKBP12)-rapamycin-binding (FRB) domain of mammalian target of rapamycin (mTOR) and thus regulate its activity (9–11). We hypothesized that there may be different molecular species of PA that modulate mTORC1 or mTORC2 activities, thereby regulating insulin signaling and

hepatic gluconeogenesis. In this study, we determined the molecular species of endogenous LPA and PA in livers of *Agpat2*$^{-/-}$ mice and tested the effects of these PAs on glucose and lipid metabolism in primary hepatocytes. When the primary hepatocytes were incubated with PAs, we observed increased glucose output, an effect that was inhibited by insulin in WT but not in primary hepatocytes obtained from *Agpat2*$^{-/-}$ mice. Thus, our study shows for the first time that PAs alter hepatic gluconeogenesis.

EXPERIMENTAL PROCEDURES

Animals—All animal studies were approved by the Institutional Use and Care of Animals and BioSafety Committee at the University of Texas Southwestern Medical Center.

Isolation, Separation, and Quantification of Total LPA and PA by High Performance Liquid Chromatography (HPLC) from Mouse Livers—The extraction of LPA and PA was performed as described previously (12). Approximately 250 mg of liver from 4-month-old WT or *Agpat2*$^{-/-}$ mice from C57BL/6 and 129Sv mixed background was homogenized in 100 mM Tris-HCl, pH 7.5, containing 10 mM NaCl. Cellular debris was removed by centrifugation at $3000 \times g$ for 5 min at 4 °C and an aliquot was used to extract DNA. DNA was extracted with Easy-DNA kit (Invitrogen) following the manufacturer's protocol. A known volume of the homogenate was used to extract total LPA and total PA using 1-butanol, 1 N HCl as reported elsewhere (13). The upper aqueous phase was removed and the extraction was repeated twice with water-saturated butanol (4:1) and the upper aqueous phase was combined with the previous extract and dried under vacuum. The dried phospholipid extracts were resuspended in a known volume of chloroform. LPA and PA standards were resolved using a gradient solvent system: Buffer A, chloroform/methanol/water/ammonium hydroxide (80:19.5:0:0.5, v/v) and Buffer B, chloroform/methanol/water/ammonium hydroxide (60:34:5:0.5, v/v) (14) on a Supelcosil LC-Diol column (5 μm; 25 cm $\times$ 4.6 mm, Sigma) connected to a Waters 1525 HPLC (Waters corporation, Milford, MA) equipped with an evaporative light scattering detector (Waters 2420). Standard curves were generated for LPA and PA and used to determine the concentration of liver LPA and PA using Breeze software (version 3.30 SPA). Standard phospholipids 1-oleoyl-2-hydroxy-*sn*-glycero-3-phosphate (LPA) and 1,2-dioleoyl-*sn*-glycero-3-phosphate (PA) were from Avanti Polar Lipids (Alabaster, AL). The concentrations of LPA and PA were normalized to DNA.

Digestion of Total PA with Phospholipase A$_2$ (PLA$_2$) and Methylation of Free Fatty Acids—The total PA (200 μg) extracted from the livers of WT and *Agpat2*$^{-/-}$ mice was vacuum dried and resuspended in 50 μl of PLA$_2$ assay buffer (50 mM Tris-HCl, 100 mM NaCl, 1 mM CaCl$_2$, pH 8.9) and digested with 1.6 units of PLA$_2$ from snake venom (Worthington) for 20 min at 25 °C. The digested samples were spotted on Silica Gel 60 Å thin layer chromatography (TLC) glass plates. The LPA, PA, and fatty acids were resolved using the solvent system chloroform/methanol/acetic acid/water (25:10:3:1, v/v) and visualized in iodine vapors. The released free fatty acids were transmethylated as described previously with slight modifications (15). The spots corresponding to free fatty acids were scraped

and suspended in 2 ml of methanol/hexane (4:1, v/v) containing 200 μl of acetyl chloride, and the mixture was heated at 100 °C for 1 h. The samples were cooled to room temperature (RT) and 6% potassium carbonate was added. The methyl esters of fatty acids were extracted in hexane. The hexane extracts were analyzed on an Agilent 6890 gas chromatographic (GC) system equipped with a flame ionization detector under the following conditions: a DB-23 (HP-5ms, 30 m, 0.25 mm, 0.25 μm, Agilent) capillary column was used with hydrogen (2 ml/min) as carrier gas. Helium was used as the makeup gas. The temperature of the oven was maintained at 225 °C for 3 min, and then raised to 265 °C for 20 min. An Agilent gas chromatography fitted with a split/splitless injection system was used with the split ratio set to 50:1. The flame ionization detector was maintained at 300 °C. The concentration of various fatty acids was determined by the peak area of the fatty acid methyl esters with Agilent G1701DA GC/MSD ChemStation software (version D.00.00.38). The percent recovery of each fatty acid was normalized to C19:0 used as an internal standard (Avanti Polar Lipids).

Phospholipid Analysis by Mass Spectrometry—An automated electrospray ionization-tandem mass spectrometry was used, and data acquisition and analysis were carried out as described previously (16) with few modifications. The dried fractions of LPA (10 μg) and PA (10 μg) were resuspended in chloroform. C13:0/LPA (0.4 nmol), C14:0/LPA, and C17:1/PA (0.3 nmol) (Avanti Polar Lipids) were added as internal standards. This was combined with solvents such that the ratio of chloroform, methanol, 300 mM ammonium acetate in water was 300:665:35. LPA and PA fractions were introduced by continuous infusion into the ESI source on a triple quadrupole MS/MS (4000QTrap, Applied Biosystems, Foster City, CA). Samples were introduced using an autosampler (LC Mini PAL, CTC Analytics AG, Zwingen, Switzerland) fitted with the required injection loop for the acquisition time and presented to the ESI needle at 30 μl/min.

Sequential precursor and neutral loss scans of the LPA and PA fractions, respectively, produced a series of spectra with each spectrum revealing different molecular species of LPA and PA. LPA species were detected in negative mode $[M - H]^-$ with precursor 152.9; PA was detected in positive ion mode $[M + NH_4]^+$ with neutral loss 115.0. The scan speed was 100 units/s. The collision gas pressure was set at 2 (arbitrary units). The collision energies, with nitrogen in the collision cell, were $+25$ V for PA and -51 V for LPA. Declustering potentials were $+100$ V for PA and -100 V for LPA. Entrance potentials were $+14$ V for PA and -10 V for LPA. Exit potentials were $+14$ V for PA and -14 V for LPA. The mass analyzers were adjusted to a resolution of 0.7 unit of full width at half-height. For each spectrum, 200 to 400 continuum scans were averaged in multiple channel analyzer mode. The source temperature (heated nebulizer) was 100 °C, the interface heater was on, $+5.5$ kV or -4.5 kV were applied to the electrospray capillary, the curtain gas was set at 20 (arbitrary units), and the two ion source gases were set at 45 (arbitrary units). The background of each spectrum was subtracted, the data were smoothed, and peak areas were integrated using a custom script and Applied Biosystems Analyst software. After isotopic deconvolution, the various molecular species of LPA and PA were quantified in

TABLE 1
Primers used in this study

Target mRNA	Forward primer	Reverse primer
Acc1	TGGACAGACTGATCGCAGAGAAAG	TGGAGAGCCCCACACACA
Fas	GCTGCGGAAACTTCAGGAAAT	AGAGACGTGTCACTCCTGGACTT
G6pase	TGGGCAAAATGGCAAGGA	TCTGCCCCAGGAATCAAAAAT
Pepck	CCACAGCTGCTGCAGAACA	GAAGGGTCGCATGGCAAA
Pld1	TTCGAGGGAGACATTTCCAC	TTCCAGCTCTGCATGTGTTC
Pld2	TGTTGGAGTGGTTGTACACG	CATGAAGGGGAGATTGTTTG
Pld3	GTAGCAGCCAACGTCTGATT	TTCATTCAAGGGCAGTTCTC
Pld4	AACCACAGCAAGTTCATGGT	GCTCGGGACTTGTCTGTCTA
Pld5	TGTGCAACGAAAGAACAAAA	TGCTCCTGTTGTCTCTCACA
Pld6	CTCTCCTGGGCATCACTAGA	CAAGTCCACAGTCTGGCTCT
Dagk1	GGCTGAGAAGACCAAGTCAA	TCTAGATATTCGGCCACTCG
Dagk2	GCCACCTACCACAATCTGTC	AACTAGAAGCGGATGTGTGC
Dagk3	GAATGTTCTCTGTGCCTGCT	CCTAAGCAGGAGGACTTTCC
Dagk4	AGCGAAAAGTGTGACTTTGG	TCAAACACCTGGACTGGATT
Dagk5	AGTGTTGCATGGTGAGGAAT	CTCATCTTTCAGCCGAGTGT
Dagk6	GTCTTGGGAAGACAAGCAGA	GCTGCGTCACAAATCCTAGT
Dagk7	GAAAGACTTCAGCCACTCCA	TCCGTGGTCAAGGATGTACT
Dagk8	GGGACCTTGATTGGCTTTAT	TGAGGACTGGTGTTCCATTT
Dagk9	GTCCAAAAATGAGCTGCCTA	ACACACAGGAGAAGGCTCTG
Dagk10	AGAAGCCAACCCAGAGAAGT	CTGAATCTTGGGGGTTAGGT
G6pase	CGACGCGTCATGAACAAGGGCATGACTG	CCGCTCGAGTCGGGATGGTTCTTACCACT
Pepck	CGACGCGTGGGCAAGAAATCACCAAAGA	CCGCTCGAGGGGACTCACCAGTTGTCATATTT

comparison to the internal standards of that class (17). To correct for chemical or instrumental noise in the samples, the molar amount of each phospholipid detected in the "internal standards only" spectra was subtracted from the molar amount of each metabolite calculated in each set of sample spectra. The data were also corrected for the fraction of the sample analyzed from the HPLC. Based on this data, the total amount of individual LPA and PA species was calculated and normalized to DNA.

Saturation Curves for Phospholipase D (Pld) and Diacylglycerol Kinase (Dagk) Enzymes—PLD assay was performed using different concentrations of the substrate C18:1/18:1 PC from 0.0038 to 1.272 μM. DAGK assay was performed using different concentrations of the substrate C18:1/18:1 DAG from 0.0048 to 0.61 μM.

Phospholipase D (PLD) Activity in Liver Homogenates—The PLD assay was carried out as described previously (18). The assay reaction (200 μl) contained 50 mM Hepes-KOH, pH 7.5, 250 mM sucrose, 80 mM potassium chloride, 4.5 mM magnesium chloride, 3 mM calcium chloride, 3 mM EGTA, 1 mM dithiothreitol, protease inhibitors, and 100 μM GTP. Enzymatic reaction was started by adding 100 μg of whole cell lysate. The substrate was provided as mixed micelles of 0.012 μM 1,2-dioleoyl-*sn*-glycero-3-phosphocholine (C18:1/18:1 phosphatidylcholine) and [^{3}H]1,2-distearoyl-*sn*-glycero-3-phosphocholine (C18:0/18:0 phosphatidylcholine) (American Radiolabeled Chemicals. Inc., St. Louis, MO) prepared by evaporating the chloroform and resuspending in the assay buffer. The reactions were incubated at 37 °C for 30 min. Enzymatic reactions were stopped by addition of 1 ml of chloroform/methanol/concentrated HCl (50:50:0.3) and 0.35 ml of 1 M HCl, 5 mM EDTA, followed by vigorous mixing. After centrifugation at 1000 × *g* for 10 min at 4 °C, the lower organic phase was recovered and the above extraction was repeated twice. The lower phases were combined and dried under a stream of N$_2$ gas. Dried lipid films were resuspended in chloroform and spotted onto Silica Gel G-60 plates along with C18:1/18:1 PA standard (Avanti Polar Lipids). Plates were run using a solvent system of chloroform/methanol/acetic acid/water (25:10:3:1, v/v) and developed with iodine
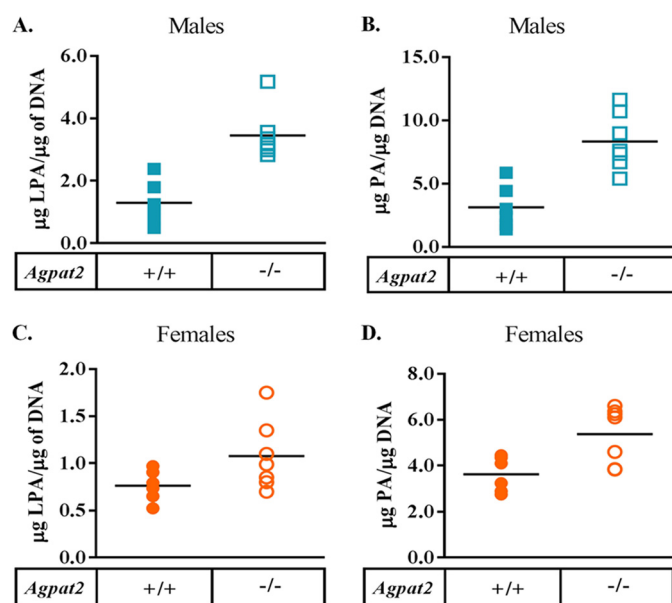

FIGURE 1. **Quantification of LPA and PA in the livers of wild type (WT) and *Agpat2*$^{-/-}$ mice.** LPA and PA were extracted from the livers of 4-month-old WT and *Agpat2*$^{-/-}$ male and female livers. *A* and *B,* LPA and PA levels in WT and *Agpat2*$^{-/-}$ male livers normalized to DNA. Shown are individual LPA and PA values, *n* = 6. The *p* value for LPA and PA was <0.01. *C* and *D,* LPA and PA levels in WT and *Agpat2*$^{-/-}$ female livers normalized to DNA. Shown are individual LPA and PA values, *n* = 6. *p* value for PA = 0.01.

vapors. The bands corresponding to PA were scraped and the radioactivity was determined by liquid scintillation.

Diacylglycerol Kinase (Dagk) Activity in Liver Homogenates—DAGK assay was carried out as described previously with slight modifications (19). The enzymatic reaction was assembled in 150 μl containing 50 mM Tris acetate, pH 7.4, 10 mM magnesium acetate, 80 mM KCl, 2 mM EGTA, 0.016 μM 1,2-dioleoyl-*sn*-glycerol (DAG), and 20 μM ATP. The stock solution of DAG in chloroform was dried under a nitrogen stream; resuspended in a small volume of 50 mM Tris acetate, pH 7.4, 10 mM magnesium acetate, 80 mM KCl, and 2 mM EGTA; and sonicated in a water bath for 15 min before being added to the reaction mixture. The enzymatic reaction was started by adding 1 μCi of
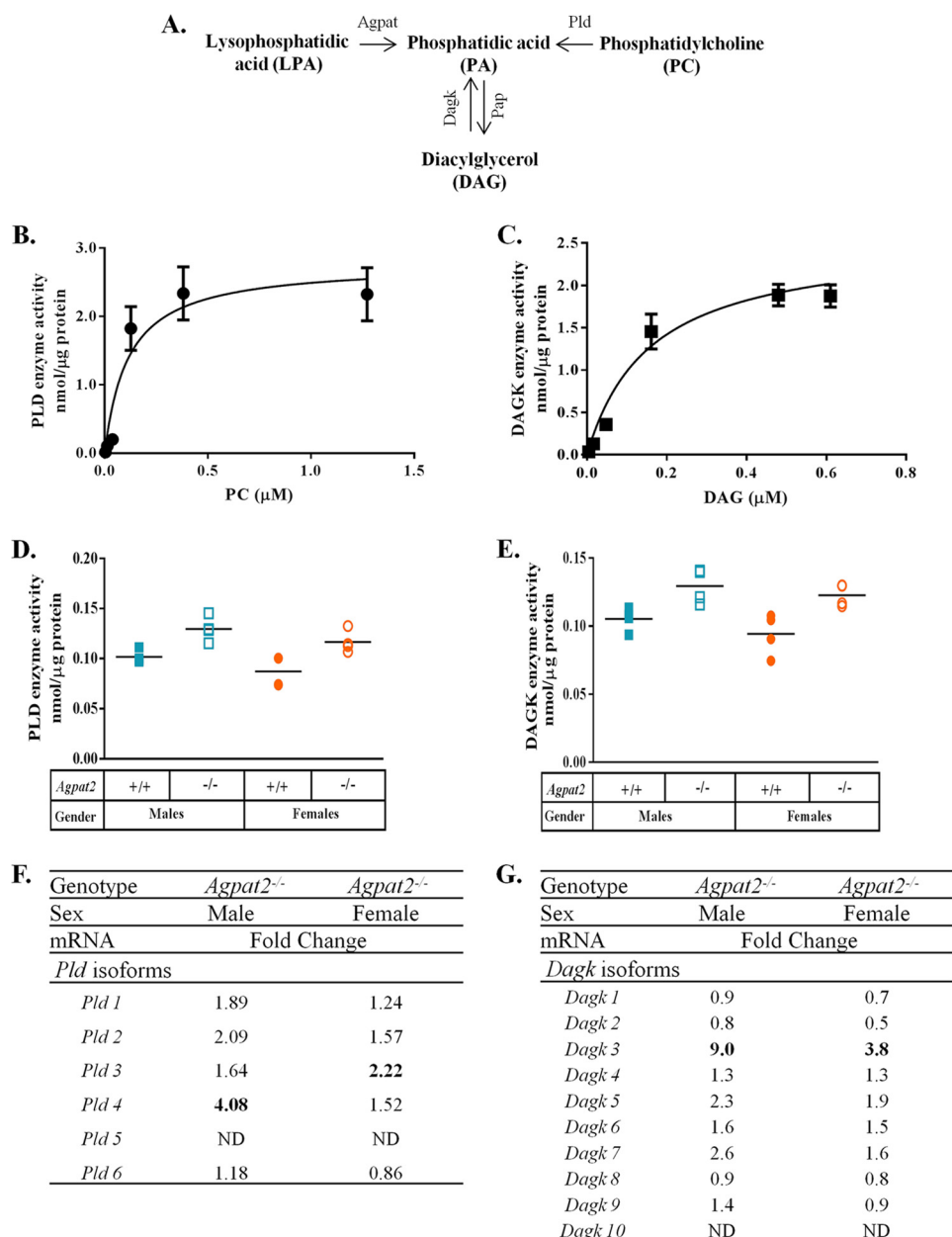
FIGURE 2. **Increased levels of PA in the livers of male and female *Agpat2*$^{-/-}$ mice may be due to alternate pathways.** *A*, schematic representation of the various pathways resulting in the synthesis of PA. PA can be generated by enzymes 1-acylglycerol-3-phosphate-*O*-acyltransferase (AGPAT), phospholipase D (PLD), and diacylglycerol kinase (DAGK). *B*, saturation curve for PLD enzyme. The apparent rate constants (V_{max}) and the apparent affinity constant (Michaelis-Menten, K_m) for PLD were determined from three individual livers and performed in triplicates ($n = 3$). V_{max} was expressed as nanomole/μg of protein and K_m was expressed as micromolar. *C*, saturation curve for DAGK enzyme. V_{max} and K_m for DAGK enzyme were determined from three individual livers and performed in triplicates ($n = 3$). V_{max} was expressed as nanomole/μg of protein and K_m was expressed as micromolar. *D*, PLD enzyme activity determined by the conversion of [^{3}H]phosphatidylcholine to [^{3}H]PA and expressed as nanomole of PA/μg of protein from liver lysates. Assays were performed with individual livers in duplicates ($n = 4$). The data indicate a statistically significant increase in PLD activity in the livers of *Agpat2*$^{-/-}$ mice compared with the WT of both genders with a *p* value of 0.012 in males and 0.023 in females. *E*, DAGK enzyme activity was determined by the conversion of 1,2-dioleoylglycerol to [^{32}P]PA in the presence of [γ-^{32}P] ATP and expressed as nanomole of PA/μg of protein from liver lysates. Assays were performed with individual livers in duplicates ($n = 4$). The data indicate a statistically significant increase in DAGK activity in the livers of *Agpat2*$^{-/-}$ mice compared with the WT of both genders with a *p* value of 0.03 in males and 0.024 in females. *F* and *G*, Q-PCR of various isoforms of *Pld* and *Dagk* analyzed in pooled samples ($n = 6$) from the livers of both genders of *Agpat2*$^{-/-}$ mice normalized to cyclophilin and expressed as a fold-change relative to WT mice. *Pld3* was up-regulated in females, whereas *Pld4* was up-regulated in males. *Dagk*3 was significantly up-regulated in the livers of both the genders. *ND*, not detected.

[γ-^{32}P]ATP (PerkinElmer Life Sciences) and 50 μl of total protein. Standard assays were performed for 30 min at RT. PA was extracted by the addition of 500 μl of 1-butanol, 1 N HCl. After centrifugation at 1000 $\times$ *g*, the aqueous layer was recovered, dried under a stream of nitrogen, dissolved in a known volume of chloroform/methanol (2:1), and applied to Silica Gel G-60

plates along with the C18:1/18:1 PA standard. Plates were developed with a solvent system of chloroform/methanol/acetic acid/water (25:10:3:1) and visualized in iodine vapors. Lipids were identified by iodine staining, labeled PA spots were scraped off, and the radioactivity was determined by liquid scintillation.
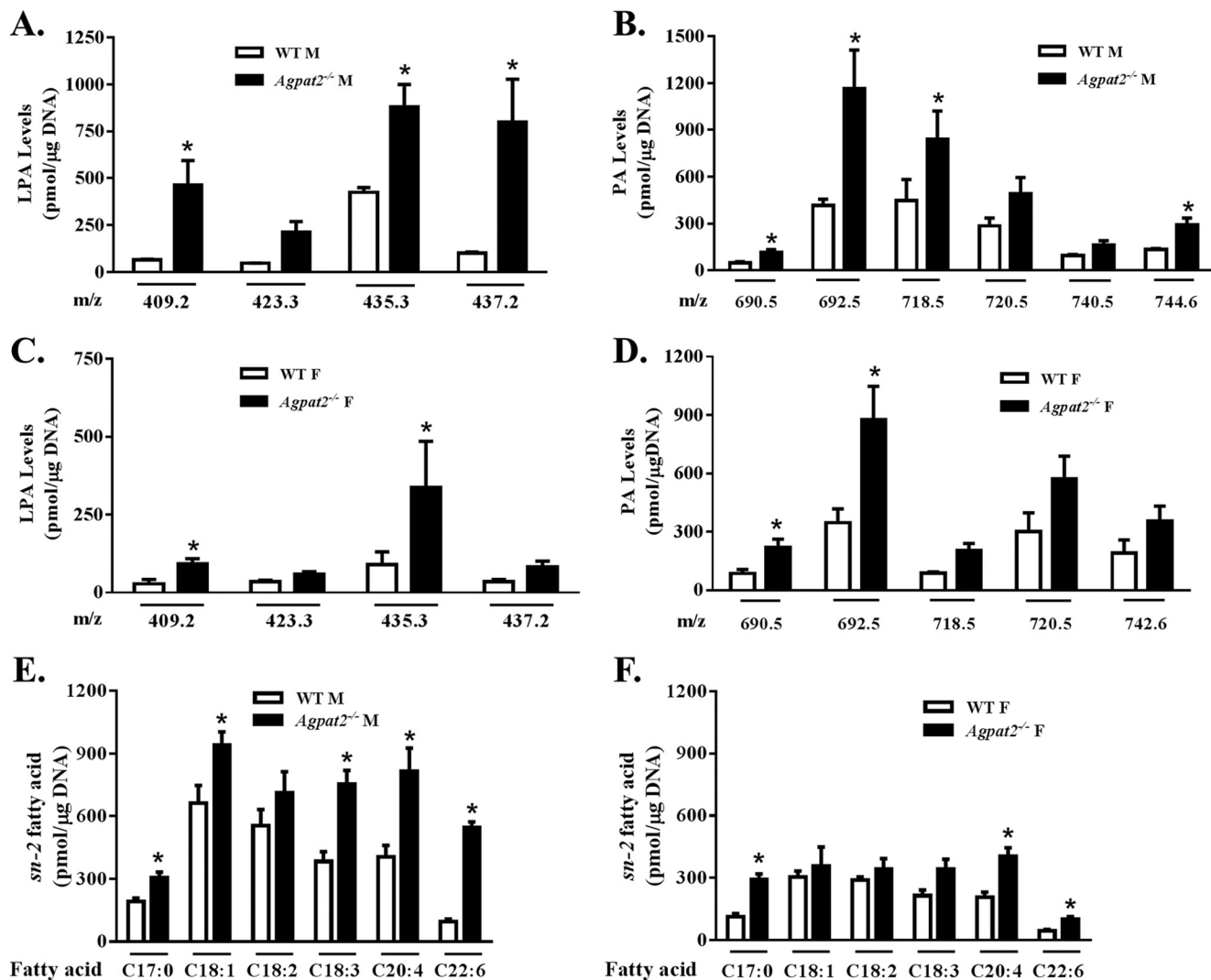
FIGURE 3. **Determination of molecular species of LPA and PA in the livers of wild type and *Agpat2*$^{-/-}$ mice.** *A–D*, charge-to-mass ratio (*m/z*) of various LPAs and PAs obtained from mass spectrometry (MS/MS) analysis. LPA and PA fractionated by HPLC were used for MS/MS analysis. LPA and PA levels are expressed as picomole/μg of DNA normalized to C13:0-LPA and C14:0, 17:1-PA (mean ± S.E.; *n* = 4 in each group). Although no distinct molecular species of PA were detected in the livers of *Agpat2*$^{-/-}$ mice, PA species 34:2, 34:2, 36:4, 36:3, 36:2, and 38:3 were found to be significantly increased in the livers compared with WT. *E* and *F*, levels of various fatty acids released upon digestion of extracted PA with PLA$_2$. The released fatty acids were extracted with methanol/hexane (1:2, v/v). The dried lipid extract was resolved on TLC and the released fatty acid was methylated and resolved using gas chromatography. Fatty acids are expressed as picomole of free fatty acid/μg of DNA. All fatty acids were normalized to C19:0 fatty acid as the internal control (mean ± S.E.; *n* = 4 in each group). Based on *m/z* and *sn*-2 fatty acids four PAs, C16:0/18:2 PA, C16:0/18:1 PA, C18:0/20:3 PA, and C18:1/20:4 PA, were statistically significant. *, *p* value ≤ 0.05.

Isolation of Mouse Primary Hepatocytes—Primary hepatocytes were isolated from 1-month-old non-fasted mice of both genders by a two-step collagenase perfusion method as described earlier (20, 21). Briefly, mice were anesthetized with isoflurane and a catheter (24 × 3/4 inch safelet catheter, Fisher Scientific) was inserted in the portal vein. The liver was perfused with the liver perfusion medium (Life Technologies) maintained at 37 °C using a peristaltic pump at a rate of 3 ml/min until the liver blanched. The liver was then perfused with the liver digest medium (Life Technologies) at a rate of 3 ml/min for 20 min, excised from the animal, and placed in a Petri dish containing the liver digest media at 37 °C. Hepatocytes were released by removing the hepatic capsule and then passed through a 100-μm cell strainer. The cells were washed three times in low glucose DMEM containing 100 mM Hepes by centrifuging at 25 × *g* for 2 min at 4 °C. The cell pellet was resuspended in low glucose DMEM

containing 10% FBS and 1% antibiotics. Approximately 1 × 10^6 cells were seeded into each well of a collagen-coated 6-well plate (Fisher Scientific) and allowed to attach overnight. The following day cells were prepared for various experiments as described.

Preparation of Liposomes with PA and Transfection of Primary Mouse Hepatocytes—Liposomes were prepared fresh for each experiment. 100 μM C16:0/18:1, C16:0/18:2, or C18:1/20:4 PA and 0.1 μCi of [³H]oleoyl-LPA (PerkinElmer Life Sciences) were dried and resuspended in PBS. The mixture was sonicated for 15 min and the liposomes were used in cell culture experiments.

Immunoblot Analysis—The hepatocytes were lysed in lysis buffer (150 mM NaCl, 50 mM Tris, pH 8.0) containing protease and phosphatase inhibitors (Roche Diagnostics). Cells were sonicated for 15 s with an interval of 1 min and centrifuged at 16,000 × *g* for 15 min at 4 °C. The whole cell lysate

proteins (75 μg) from the hepatocytes were resolved on a precast 7.5 or 10% SDS-PAGE (Bio-Rad) followed by transfer onto PVDF membranes (Millipore, Billerica, MA). The membranes were blocked with 5% nonfat dry milk containing 0.2% Tween 20 and then incubated with the primary antibody. Immunoblot analysis was carried out by following the procedures recommended by antibody suppliers.

The antibodies to total mTOR, mTORC1 (Ser-2481), mTORC2 (Ser-2448), total S6K, pS6K (Thr-389), and pAkt (Thr-308) were from Cell Signaling Technology and used at a dilution of 1:1000 at 4 °C overnight; total Akt and pAkt (Ser-473) were from Santa Cruz Biotechnology and used at a dilution of 1:200 at RT for 1 h. All blots were incubated with secondary antibody to IgG (goat anti-rabbit IgY conjugated to horseradish peroxidase (HRP)) at a 1:5000 dilution for 1 h at RT (Santa Cruz Biotechnology) and detected with Immobilon Western chemiluminescent HRP substrate (Millipore, Billerica, MA) and exposed onto x-ray films. The same blot was stripped using Restore Western blot stripping buffer (Pierce), according to the manufacturer's protocol, and re-probed with GAPDH antibody at 1:5000 dilution (mouse monoclonal, Ambion, Austin, TX). Each blot was stripped and reprobed with GAPDH considering that the protein concentration may vary from blot to blot. Films were scanned and band densities were determined with ImageJ 1.45s and normalized to GAPDH.

Quantitative Real-time PCR in Livers of WT and Agpat2$^{-/-}$ Mice—All Q-PCR were carried out in a 20-μl reaction volume in 96-well plates using the ABI PRISM 7700 sequence detection system (Applied Biosystems) as reported previously (7). Q-PCR was performed in duplicate and the transcript levels were normalized to cyclophilin. Primers used are listed in Table 1.

Glucose Output Assay—Hepatocytes isolated from the livers of 1-month-old WT or *Agpat2$^{-/-}$* mice were plated on collagen-coated 6-well plates and allowed to attach overnight. Cells were starved for 1 h by incubating in phenol red-free, glucose-free DMEM (Sigma). Cells were incubated in media containing sodium pyruvate and sodium lactate for 6 h. Before the end of 6 h, the cells were incubated with 100 μM PA (C16:0/18:1; C16:0/18:2, and/or C18:1/20:4 PA) or LPA (16:0 LPA and/or 18:1 LPA) for 30 min and 100 nM insulin for 10 min. Culture media was collected and glucose was measured using a colorimetric assay kit from Cayman Chemical (Ann Arbor, MI). The glucose output rate was normalized by cellular protein content.
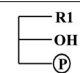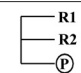
Reporter Gene Constructs—The 5′-flanking region of the glucose 6-phosphatase (*G6pase*) gene from nucleotide −1974 up to +246 and the phosphoenolpyruvate carboxykinase (*Pepck*) gene from nucleotide −2296 up to +233 was amplified from mouse genomic DNA. The PCR products were gel purified and ligated into pDrive. The insert was released from the recombinant clones by digesting them with MluI and ligated into MluI-digested pGL3 basic vector. Recombinant clones, pGL3-*G6pase* and pGL3-*Pepck*, were amplified and isolated by extraction kit from Qiagen (Valencia, CA). Primers used are listed in Table 1.

Transient Transfection of Primary Mouse Hepatocytes—Primary hepatocytes isolated from 1-month-old WT and *Agpat2$^{-/-}$* mice were co-transfected with 2 μg/well of pGL3-*G6pase* or pGL3-*Pepck* along with 0.1 μg/well of pRL-Luc using

TABLE 2

The predicted species of LPA and PA in *Agpat2$^{-/-}$* male and female livers

The table displays all the LPA and PA molecular species predicted by mass spectrometry. Also listed are the *sn-2* fatty acids obtained by cleaving PA with the PLA2 enzyme. Based on the predicted LPA and PA species from mass spectrometry and the fatty acids from PLA2 digestion, the expected PA species have been derived. The PA species that were statistically significant are shown in bold.

LPA m/z	Presumed LPA >50 pmol	PA m/z	Presumed PA >100 pmol	sn-2 fatty acids released by PLA2	PA species derived from m/z and sn-2 fatty acid
409.2	C16:0	690.5	C16:0/18:2		C16:1/20:4
423.3	C17:0	692.5	C16:0/18:1; C17:1/17:0		C16:1/18:3
435.3	C18:1	718.5	C18:1/18:1		C16:0/22:6
437.2	C18:0	720.5	C18:0/18:1		C16:0/20:4
		740.5	C18:1/20:4	17:0	C16:0/18:3
		744.6	C20:2/18:1; C18:0/20:3	18:3	**C16:0/18:2**
LPA <50 pmol		PA <100 pmol		18:2	**C16:0/18:1**
407.2	C16:1	686.5	C16:1/18:3	18:1	C18:1/22:6
421.2	C17:1	688.5	C16:0/18:3	20:4	**C18:1/20:4**
433.2	C18:2	712.5	C18:2/18:3; C16:1/20:4	22:6	C18:1/18:3
449.3	C19:1	714.5	C16:0/20:4; C18:2/18:2		C18:1/18:2
451.3	C19:0	716.5	C18:1/18:2; C18:0/18:3		C18:1/18:1
457.2	C20:4	738.5	C16:0/22:6; C18:2/20:4		C18:0/22:6
481.2	C22:6	742.5	C18:0/20:4		C18:0/20:4
483.3	C22:5	746.6	C18:1/20:1; C18:0/20:2		C18:0/18:3
485.3	C22:4	764.5	C18:1/22:6		C18:0/18:2
487.3	C22:3	766.5	C18:0/22:6		C18:0/18:1
489.3	C22:2	768.6	C20:1/20:4		**C18:0/20:3**
491.3	C22:1				

Lipofectamine 2000 following the manufacturer's protocol (Life Technologies). Cells were starved in phenol red-free, glucose-free DMEM for 1 h and incubated in DMEM containing sodium pyruvate and sodium lactate for 6 h. Before the end of the 6-h incubation, cells were supplemented with 16:0/18:1, 18:1/20:4, or 16:0/18:2 PA for 30 min and insulin for 10 min. Cell lysates were collected and a dual luciferase assay was performed. The relative luciferase activity was normalized to protein.
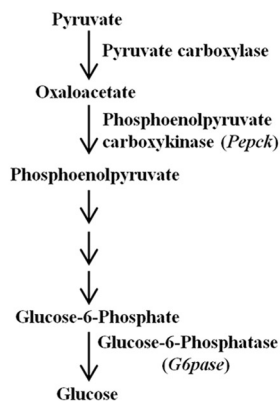
Statistical Analyses—Statistical significance was calculated either by Student's t test or two-way analysis of variance using GraphPad Prism version 5.00 for Windows. A p value less than 0.05 is considered statistically significant.
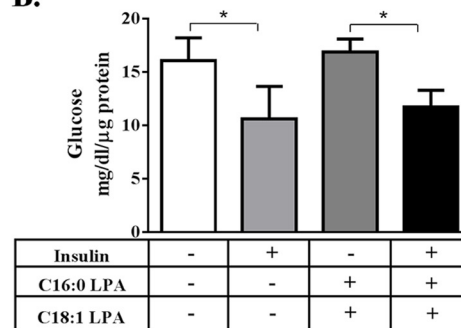
RESULTS

LPA and PA Levels Are Elevated in Livers of Agpat2$^{-/-}$ Mice—*Agpat2$^{-/-}$* mice have only ∼10% residual AGPAT activity in liver (7), whereas their total LPA and total PA remain elevated. Because AGPAT converts LPA to PA, we predicted LPA levels would be higher and PA levels would be reduced. As expected, LPA levels increased ∼2-fold in the livers of male mice (Fig. 1*A*) and female mice showed a trend toward an increase (Fig. 1*C*). However, instead of decreasing, PA levels were also increased ∼5- and ∼2-fold in the livers of male and female *Agpat2$^{-/-}$* mice, respectively (Fig. 1, *B* and *D*), indicating alternative pathway(s) exist for the synthesis of PA in the absence of *Agpat2*. In addition, we have previously reported that the levels of phosphatidylethanolamine, phosphatidylcholine, and phosphatidyl-

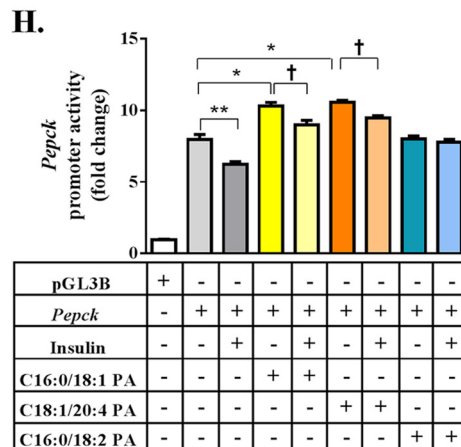serine were elevated in the livers of male $Agpat2^{-/-}$ mice but not in the livers of female $Agpat2^{-/-}$ mice (7).
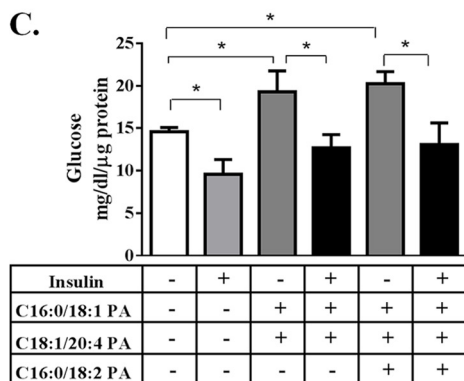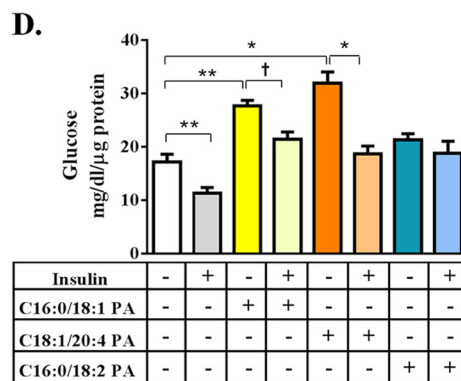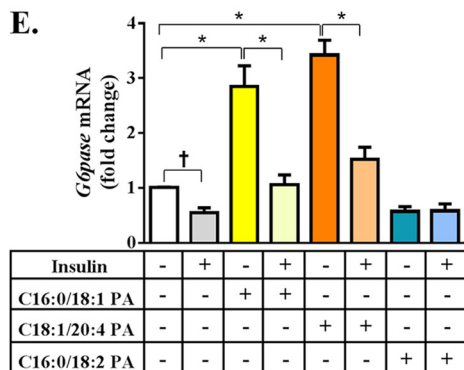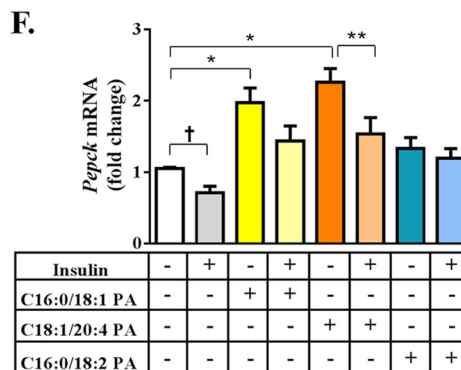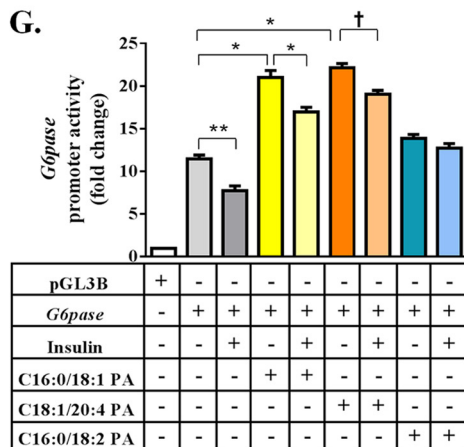
Synthesis of PA by Alternate Pathways—In the absence of AGPAT activity, mouse livers can employ alternate pathways to synthesize PA. Two families of enzymes might contribute to the synthesis of PA: phospholipase D (PLD) and diacylglycerol kinase (DAGK) (Fig. 2*A*). To determine the optimal substrate concentration for measurement of the enzymatic activity for PLD, a saturation curve was generated (Fig. 2*B*). The V_{max} and apparent K_m for PLD were 2.77 ± 0.35 nmol/μg of protein and 0.11 ± 0.05 μM, respectively. This allowed us to use the optimal substrate concentration for determining the enzymatic activity.

As shown in Fig. 2*D*, livers of $Agpat2^{-/-}$ mice had significantly higher PLD enzymatic activities. This increase in PLD enzymatic activity may be due to the ~2-fold increase in *Pld*3 mRNA levels in livers of female $Agpat2^{-/-}$ mice and the ~4-fold increase in *Pld*4 mRNA levels found in male $Agpat2^{-/-}$ mice (Fig. 2*F*).

Similarly, to determine the optimal substrate concentration for measurement of DAGK enzymatic activity, a saturation curve was generated (Fig. 2*C*). DAGK had a V_{max} of 2.54 ± 0.24 nmol/μg of protein and apparent K_m of 0.15 ± 0.04 μM. DAGK enzymatic activities in livers of $Agpat2^{-/-}$ mice of both genders were significantly increased compared with WT mice (Fig. 2*E*). We amplified all 10 *Dagk* isoforms by Q-PCR and found only *Dagk*3 was significantly increased in livers of $Agpat2^{-/-}$ mice (Fig. 2*G*). The substrate specificities for each of these enzymatic isoforms are unclear; therefore, isoform-specific substrate(s) might alter the reported activities of these enzymes in this study. However, the absolute contribution of these two pathways towards the increase of PA in the livers of $Agpat2^{-/-}$ mice remains unclear.

Molecular Species of LPA and PA in the Livers of $Agpat2^{-/-}$ Mice—Next, we determined whether there were any unique molecular species of LPA and PA generated in the livers of $Agpat2^{-/-}$ mice. The total LPA and PA samples purified by HPLC were analyzed using ESI/MS. Interestingly, we did not find any novel LPA or PA species in the livers of $Agpat2^{-/-}$ mice, although some specific LPA and PA species were elevated. The increase in m/z 409.2, 435.3, and 437.2 LPA in males (Fig. 3*A*) and m/z 409.2 and 437.2 LPA in females (Fig. 3*C*) was statistically significant. Similarly, only a few PA species were elevated compared with those of WT mice (Fig. 3, *B* and *D*). The most abundant PA species were m/z 692.5, 718.5, and 720.5 in males and m/z 692.5 and 720.5 in females, although m/z 720.5 was also elevated but not statistically significant in either gender.

Because the molecular mass obtained by ESI/MS determines both the fatty acids at the *sn-1* and *sn-2* positions of PA but not the specific fatty acid at either carbon position, we used PLA$_2$, which specifically cleaves the *sn-2* fatty acids from phospholipids, to ascertain the *sn-2* fatty acids of PAs. When the isolated total PA was digested with PLA$_2$ and analyzed by GC we detected an increase in several fatty acids (Fig. 3*E*). The largest increase was in C22:6 followed by C20:4, C18:3, C18:1, and C17:0 in male livers. In female livers we observed a statistically significant increase in C17:0, C20:4, and C22:6 fatty acids (Fig. 3*F*). Based on the m/z of the molecular species of LPA and the released fatty acid by PLA$_2$, we deduced the probable PA species (Table 2). Among the presumed PA species, the increase in m/z 690.5 (34:2 = C16:0/18:2), m/z 692.5 (34:1 = C16:0/18:1), m/z 744.5 (38:3 = C18:0/20:3), and m/z 740.5 (38:5 = C18:1/20:4) were statistically significant.

Effect of Various PA Species on Gluconeogenesis in Primary Mouse Hepatocytes—To determine whether the changes measured in LPA and PA in $Agpat2^{-/-}$ mice may affect HGP, we first added a mixture of C16:0 and C18:1 LPAs in the ratio of 1:2, as found in the livers of $Agpat2^{-/-}$ mice, to primary hepatocytes from WT mice and found no increase in HGP (Fig. 4*B*). These LPAs were tested individually and none altered HGP (data not shown), suggesting that LPA may not play any role in gluconeogenesis.

We next tested a mixture of PAs, which were significantly elevated in the livers of $Agpat2^{-/-}$ mice. C16:0/18:1 PA and C18:1/20:4 PA or C16:0/18:1 PA, C18:1/20:4 PA, and C16:0/18:2 PA in a molar ratio of 1:0.5:0.5 (as found in the livers of $Agpat2^{-/-}$ mice) were incubated with primary hepatocytes from WT mice. These PA mixtures increased HGP ~1.5-fold, an effect that was suppressed in the presence of insulin (Fig. 4*C*). A similar response was observed when $Agpat2^{-/-}$ mouse hepatocytes were tested with the same PA mixtures (data not shown). Although C18:0/20:3 PA was also significantly increased we could not test this PA as it is not commercially available and accounted for only ~1% of the total liver PA extracted from $Agpat2^{-/-}$ mice.

To determine whether the increase in HGP was specific to PA, we tested another phospholipid PC for its effect on HGP. Interestingly, C18:1/18:1 PC significantly decreased (~25%) HGP in WT primary hepatocytes, suggesting that PC is not the cause for increased HGP by PA (data not shown).

The PA species (C16:0/18:2, C16:0/18:1, and C18:1/20:4), which were significantly increased in the livers of $Agpat2^{-/-}$ mice (Table 2 and Fig. 3, *B* and *D*), were supplemented to the hepatocytes. When each individual PA species was incubated

FIGURE 4. Enhanced gluconeogenesis in primary mouse hepatocytes in the presence of PA. *A,* schematic representation of the gluconeogenesis pathway. *B,* glucose output was measured in the culture medium from the WT primary mouse hepatocytes when tested with two LPAs: C16:0-LPA and 18:1-LPA in the ratio of 1:2. *C,* glucose output was measured in culture medium from the WT primary mouse hepatocytes when tested with two PAs: C16:0/18:1 PA and C18:1/20:4 PA, or three PAs: C16:0/18:1 PA, C18:1/20:4 PA, and C16:0/18:2 PA, in molar ratios of 1:0.5:0.5. *D,* glucose output was measured in culture medium from the WT primary mouse hepatocytes when transfected with C16:0/18:1 PA, C18:1/20:4 PA, and C16:0/18:2 PA individually and expressed as milligrams/dl/μg of protein. Shown are the mean ± S.E. from six independent experiments performed in duplicate. *E* and *F,* expression of mRNA for *G6pase* and *Pepck* analyzed by Q-PCR and normalized to cyclophilin. Shown is the fold-change compared with untransfected WT primary mouse hepatocytes (expressed as mean ± S.E., $n = 4$). The expression of both *G6pase* and *Pepck* increased in the presence of C16:0/18:1 PA and C18:1/20:4 PA but this effect was nullified by insulin. *G* and *H,* change in the promoter activities of *G6pase* and *Pepck* as measured by a dual luciferase assay and expressed as fold-changes compared with pGL3 basic in primary mouse hepatocytes (expressed as mean ± S.E.). Only the PAs that activated mRNA expression of *G6pase* and *Pepck* also activated respective promoters (*G6pase*; $n = 6$ and *Pepck*; $n = 5$). The p values are shown *above* the bars: *, <0.001; **, <0.01; †, <0.05.
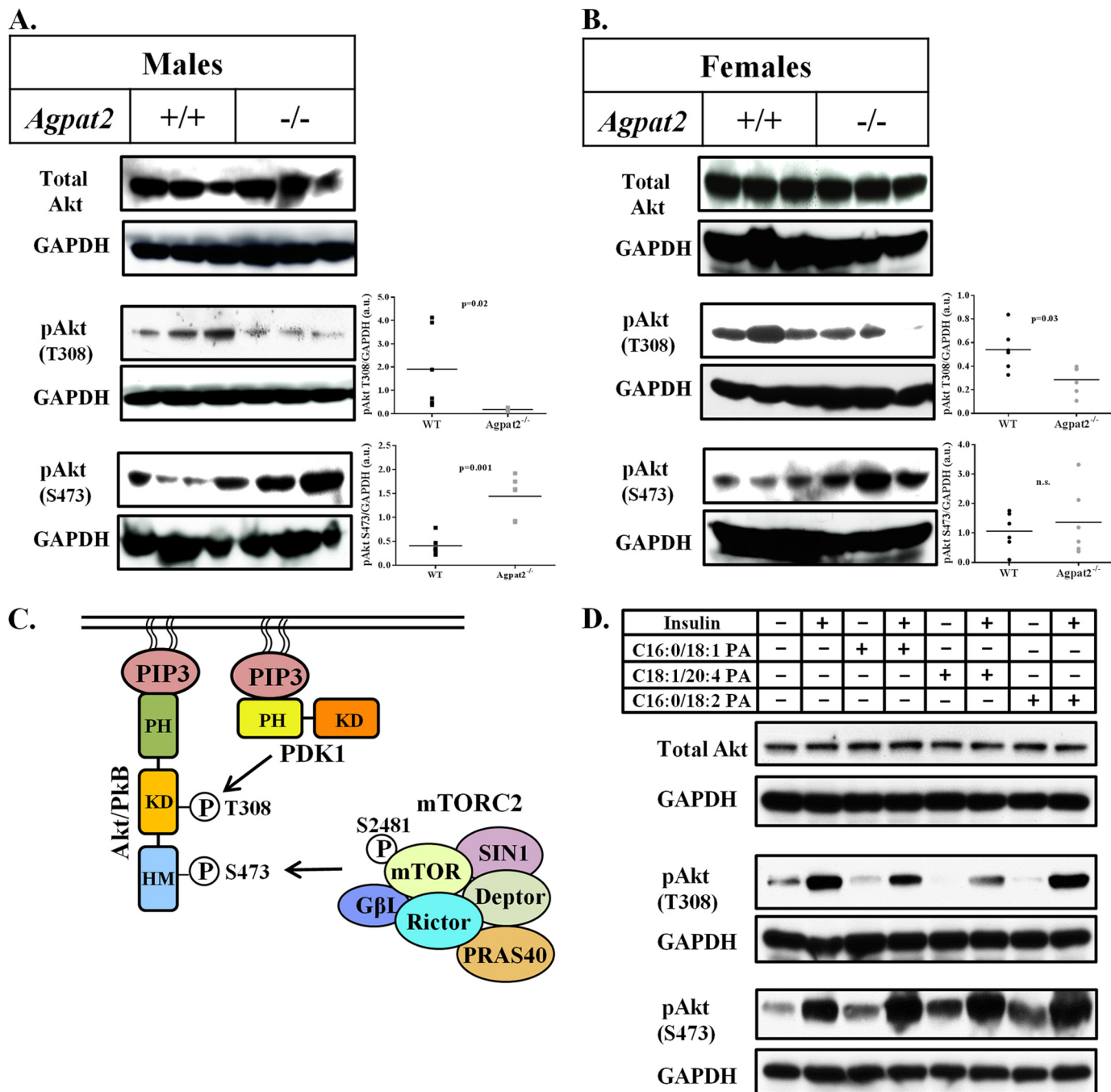
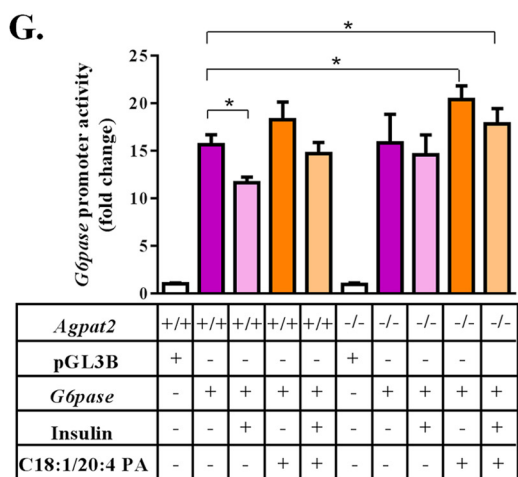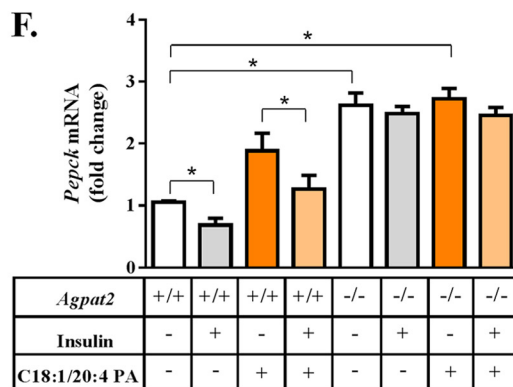FIGURE 5. **Decreased phosphorylation of Akt at Thr-308 in the livers of *Agpat2*⁻/⁻ mice suggests that PA may have a specific effect on the different phosphorylated forms of Akt.** *A* and *B*, immunoblots of Akt and its phosphorylated forms, Akt-Thr-308 and Akt-Ser-473, in the livers of male and female WT and *Agpat2*⁻/⁻ mice. Shown are representative immunoblots for total Akt, Akt-Thr-308, and Akt-Ser-473. The protein bands were normalized to GAPDH (*n* = 6). Phosphorylation of Akt at Thr-308 by PDK1 was significantly decreased in *Agpat2*⁻/⁻ mice livers compared with those of WT livers. Interestingly, phosphorylation of Akt at Ser-473 by mTORC2 was increased in the livers of *Agpat2*⁻/⁻ mice compared with WT mice. *C*, schematic representation of the PI3K-Akt pathway. PI3K catalyzes the conversion of membrane-bound PIP$_2$ (phosphatidylinositol 4,5-biphosphate) to PIP$_3$ (phosphatidylinositol 3,4,5-triphosphate). PIP$_3$ binds to the pleckstrin homology domain of Akt, which results in activation through dimerization and exposure of its catalytic site. PIP$_3$ also activates PDK1, which in turn phosphorylates Akt at Thr-308. *D*, immunoblot analysis of total Akt, pAkt-Thr-308, and pAkt-Ser-473, in the WT primary mouse hepatocytes transfected with C16:0/18:2 PA, C16:0/18:1 PA, and C18:1/20:4 PA. Total Akt remained unchanged in the presence of all three PAs. pAKT-Ser-473, a downstream target for mTORC2 remained unchanged in the presence of all three PAs but increased in the presence of insulin. Although pAkt-Thr-308 decreased in the presence of all three PAs, the phosphorylation was increased by insulin. As a loading control GAPDH was determined for each blot. Shown are representative immunoblots for total Akt, Akt-Thr-308, and Akt-Ser-473 from three independent experiments.

with primary hepatocytes, we measured a 2–2.5-fold increase in glucose output in the presence of C16:0/18:1 PA and C18:1/20:4 PA (Fig. 4*D*). The increase in HGP in the presence of C16:0/18:2 PA was not statistically significant. The increase in glucose pro-

duction induced by C16:0/18:1 PA and C18:1/20:4 PA was suppressed by insulin.

The increase in glucose production induced by a specific PA species was associated with increased expression of key genes

A. Males — μg LPA/μg DNA; *Agpat2* +/+, -/-

B. Males — μg PA/μg DNA; *Agpat2* +/+, -/-

C.

Agpat2	+/+	+/+	-/-	-/-
Insulin	-	+	-	+

Total Akt / GAPDH
pAkt (T308) / GAPDH
pAkt (S473) / GAPDH

D. Glucose mg/dl/μg protein

Agpat2	+/+	+/+	+/+	+/+	-/-	-/-	-/-	-/-
Insulin	-	+	-	+	-	+	-	+
C18:1/20:4 PA	-	-	+	+	-	-	+	+

E. *G6pase* mRNA (fold change)

Agpat2	+/+	+/+	+/+	+/+	-/-	-/-	-/-	-/-
Insulin	-	+	-	+	-	+	-	+
C18:1/20:4 PA	-	-	+	+	-	-	+	+

F. *Pepck* mRNA (fold change)

Agpat2	+/+	+/+	+/+	+/+	-/-	-/-	-/-	-/-
Insulin	-	+	-	+	-	+	-	+
C18:1/20:4 PA	-	-	+	+	-	-	+	+

G. *G6pase* promoter activity (fold change)

Agpat2	+/+	+/+	+/+	+/+	+/+	-/-	-/-	-/-	-/-	-/-
pGL3B	+	-	-	-	-	+	-	-	-	-
G6pase	-	+	+	+	+	-	+	+	+	+
Insulin	-	-	+	-	+	-	-	+	-	+
C18:1/20:4 PA	-	-	-	+	+	-	-	-	+	+

H. *Pepck* promoter activity (fold change)

Agpat2	+/+	+/+	+/+	+/+	+/+	-/-	-/-	-/-	-/-	-/-
pGL3B	+	-	-	-	-	+	-	-	-	-
Pepck	-	+	+	+	+	-	+	+	+	+
Insulin	-	-	+	-	+	-	-	+	-	+
C18:1/20:4 PA	-	-	-	+	+	-	-	-	+	+
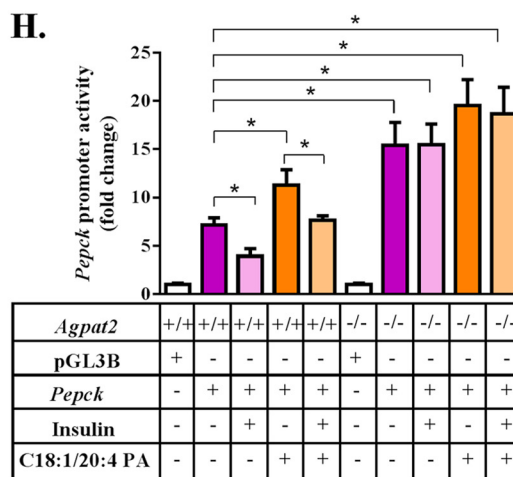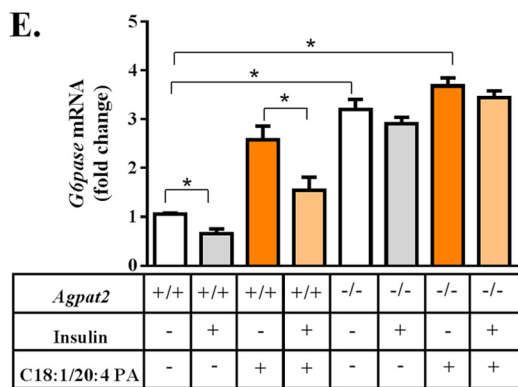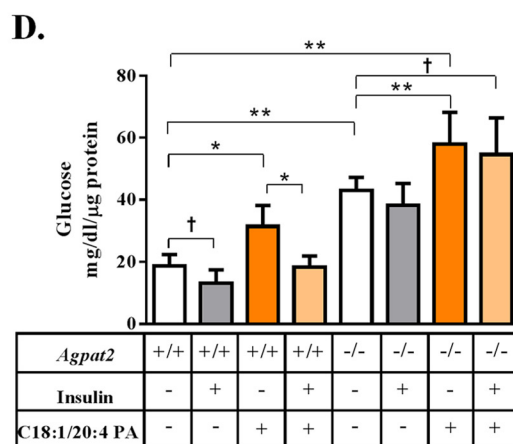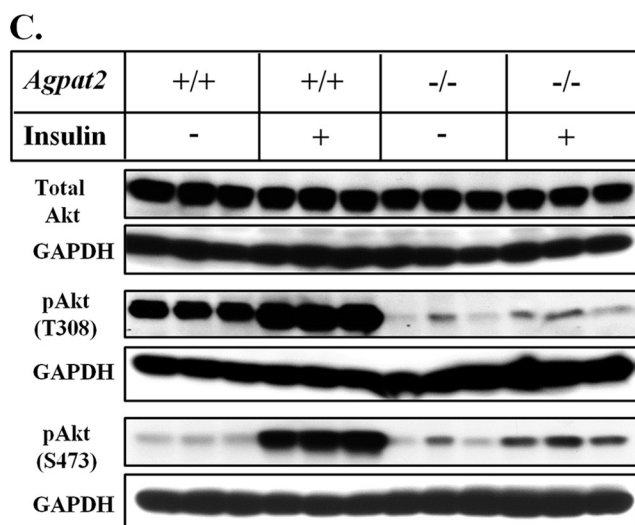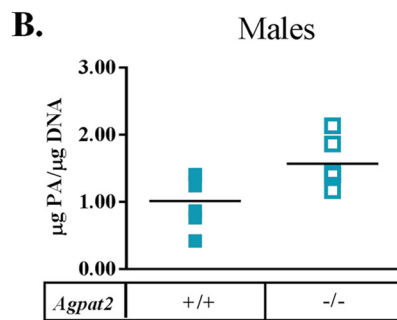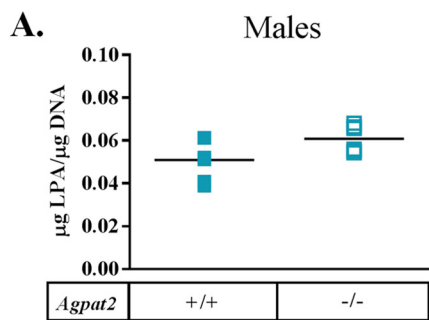
involved in glucose metabolism, *G6pase* and *Pepck* (Fig. 4, *E* and *F*). The mRNA expression of *G6pase* was increased ~2.8- and ~3.4-fold and *Pepck* increased ~2.0- and ~2.2-fold in the presence of C16:0/18:1 PA and C18:1/20:4 PA, respectively (Fig. 4, *E* and *F*).

We next determined if the increase in gene expression was transcriptionally regulated by PA. For these experiments we expressed the proximal promoter regions of *G6pase* and *Pepck* fused to a luciferase reporter gene in primary hepatocytes in the presence of PA and insulin. The relative luciferase units for *G6pase* increased ~9.5- and ~10.7-fold and *Pepck* increased ~2.3- and ~2.6-fold in the presence of C16:0/18:1 PA and C18:1/20:4 PA, respectively (Fig. 4, *G* and *H*).

Insulin-resistant Agpat2$^{-/-}$ Mouse Livers Show a Decrease in Phosphorylation of Akt at Thr-308—We next sought to determine how insulin signaling is altered in livers of *Agpat2$^{-/-}$* mice. Akt, a key component of the insulin signaling cascade, is phosphorylated by at least two kinases, 3-phosphoinositide-dependent protein kinase 1 (PDK1) at amino acid Thr-308 (22) and mTORC2 at amino acid Ser-473 (23). Surprisingly, in the livers of both genders of *Agpat2$^{-/-}$* mice, the phosphorylation of Akt at Thr-308 was significantly decreased, whereas total Akt remained unchanged (Fig. 5, *A* and *B*). This suggests that PDK1 (most likely) was not recruited by phosphatidylinositol 3,4,5-triphosphate (PIP$_3$) and thus failed to phosphorylate Akt at Thr-308. However, the phosphorylation of Ser-473 by mTORC2, which is not required to be recruited to the plasma membrane, was enhanced in livers from both genders. Despite the fact that *Agpat2$^{-/-}$* mice are highly insulin resistant, their livers still have higher PA levels, which may partially explain why the phosphorylation of mTOR and its target proteins show a slight increase in the livers of *Agpat2$^{-/-}$* mice (data not shown).

Molecular Target(s) of PA in Primary Mouse Hepatocytes That Regulate Insulin Signaling—Because mTOR was unaffected in the livers of *Agpat2$^{-/-}$* mice, we next explored the effect of PA on Akt (Fig. 5*C*). Total Akt levels remained unchanged when WT hepatocytes were incubated with C16:0/18:1, C18:1/20:4, or C16:0/18:2 PA either alone or in the presence of insulin (Fig. 5*D*). pAkt-Thr-308 levels were decreased in the presence of all three PAs but increased by insulin. The second phosphorylation site of Akt at Ser-473 remained unchanged in the presence of all three PAs and was stimulated in the presence of insulin (Fig. 5*D*).

Primary Hepatocytes Isolated from Agpat2$^{-/-}$ Mice Remain Insulin Resistant under Culture Conditions—Next, we measured LPA and PA levels in hepatocytes isolated from *Agpat2$^{-/-}$* male mice and compared them to WT male mice. Because hepatocytes may behave differently in culture compared with whole animal livers under steady state conditions, it was imperative to determine the LPA and PA levels in the hepa-

tocytes. The LPA levels showed a modest increase in hepatocytes isolated from the livers of *Agpat2$^{-/-}$* mice (Fig. 6*A*), whereas the PA levels were significantly increased (Fig. 6*B*). Similar to whole livers, the phosphorylation of Akt at Thr-308 in *Agpat2$^{-/-}$* hepatocytes was reduced compared with WT hepatocytes (Fig. 6*C*). PDK1, which seemed to be inhibited in *Agpat2$^{-/-}$* livers, was also inactive in primary hepatocytes. The phosphorylation of Akt at Ser-473 in the presence of insulin in *Agpat2$^{-/-}$* hepatocytes was markedly reduced when compared with WT hepatocytes. This suggests that the hepatocytes isolated and cultured from the livers of *Agpat2$^{-/-}$* mice still remained insulin resistant.

We next measured glucose output in the presence of C18:1/20:4 PA. The glucose output from *Agpat2$^{-/-}$* hepatocytes was higher than WT hepatocytes and C18:1/20:4 PA further increased gluconeogenesis in *Agpat2$^{-/-}$* hepatocytes (Fig. 6*D*). In contrast to WT primary hepatocytes, C18:1/20:4 PA-induced HGP was not suppressed by insulin in hepatocytes from *Agpat2$^{-/-}$* mice. The increased HGP was accompanied by increased mRNA expression of *G6pase* and *Pepck* (Fig. 6, *E* and *F*).
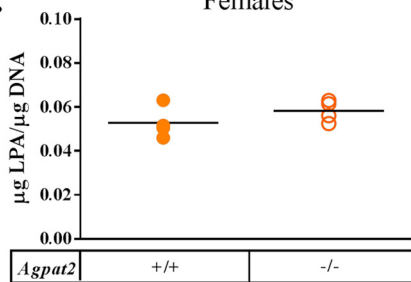
We also determined if the increase in *G6pase* and *Pepck* gene expression was transcriptionally regulated by PA. For these experiments, we expressed the proximal promoter regions of *G6pase* and *Pepck* fused to a luciferase reporter gene in primary hepatocytes in the presence of PA and insulin. The promoter activity for *G6pase* and *Pepck* was increased in the presence of C18:1/20:4 PA in hepatocytes isolated from *Agpat2$^{-/-}$* male mice compared with those from WT male (Fig. 6, *G* and *H*).

In female mice, the LPA and PA levels in primary hepatocytes were only modestly increased compared with WT mice (Fig. 7, *A* and *B*). The phosphorylation of Akt at Thr-308 in the isolated primary hepatocytes was also reduced compared with WT hepatocytes (Fig. 7*C*) suggesting that these hepatocytes also remained insulin resistant. Gluconeogenesis increased in the presence of C18:1/20:4 PA in *Agpat2$^{-/-}$* primary mouse hepatocytes but remained unchanged upon addition of insulin (Fig. 7*D*). Similar to the hepatocytes isolated from *Agpat2$^{-/-}$* male mice, the hepatocytes from *Agpat2$^{-/-}$* female mice also showed increased mRNA expression of *G6pase* and *Pepck* (Fig. 7, *E* and *F*) as well as increased promoter activity (Fig. 7, *G* and *H*) in the presence of C18:1/20:4 PA compared with the WT primary hepatocytes.
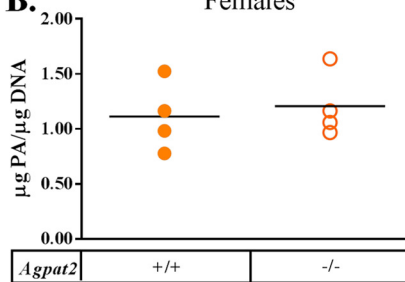
Hepatic Lipogenesis Is Independent of PA Induction—Previously, we have shown that hepatic mRNA levels of lipogenic genes acetyl-CoA carboxylase (*Acc1*) and fatty acid synthase (*Fas*) were increased in the livers of *Agpat2$^{-/-}$* mice (7). To test whether lipogenesis is also induced by PA, hepatocytes isolated from the livers of both genders of WT and *Agpat2$^{-/-}$* mice were incubated with C18:1/20:4 PA and the mRNA expression

FIGURE 6. **Primary mouse hepatocytes from *Agpat2$^{-/-}$* male mice are insulin resistant.** *A* and *B*, quantification of LPA and PA in primary mouse hepatocytes isolated from WT and *Agpat2$^{-/-}$* male mice. The LPA remained unchanged in *Agpat2$^{-/-}$* primary mouse hepatocytes when compared with WT hepatocytes. The PA levels showed a significant increase. Shown are means for LPA and PA. *p* value for PA levels = 0.03, *n* = 6. *C*, immunoblotting of Akt and its phosphorylated forms, Akt-Thr-308 and Akt-Ser-473, in primary mouse hepatocytes. Shown are representative immunoblots of total Akt and pAkt-Thr-308 and pAkt-Ser-473 from three independent mice. *D*, glucose output in primary hepatocytes from *Agpat2$^{-/-}$* male mice. Shown are the mean ± S.E. (*n* = 6) performed in duplicate. C18:1/20:4 PA increased the glucose output in primary hepatocytes from *Agpat2$^{-/-}$* male mice, and insulin was unable to suppress gluconeogenesis. *E* and *F*, fold-change (expressed as mean ± S.E., *n* = 4) of *G6pase* and *Pepck* normalized to cyclophilin. The expression of both gluconeogenic genes was increased in the presence of C18:1/20:4 PA. Insulin failed to suppress gluconeogenesis. *G* and *H*, change in promoter activity of *G6pase* and *Pepck* as measured by dual luciferase assay and expressed as fold-change compared with pGL3 basic in primary mouse hepatocytes from *Agpat2$^{-/-}$* male mice (expressed as mean ± S.E., *n* = 4). The *p* values are shown *above* the *bars* (*, <0.001; **, <0.01; †, <0.05).
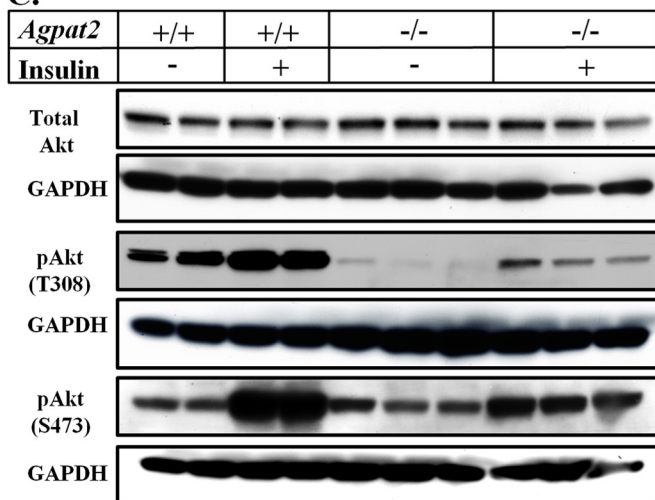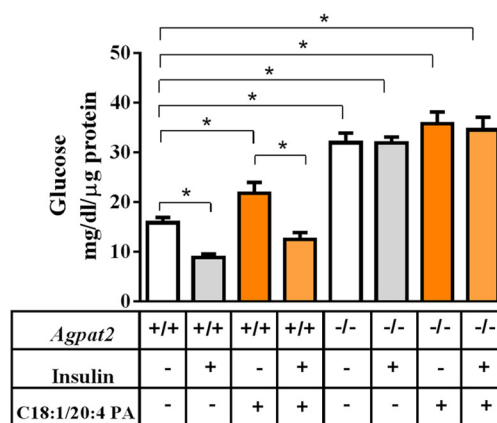
A. Females — μg LPA/μg DNA vs *Agpat2* (+/+, -/-)

B. Females — μg PA/μg DNA vs *Agpat2* (+/+, -/-)

C.

Agpat2	+/+	+/+	-/-	-/-
Insulin	-	+	-	+

Total Akt / GAPDH / pAkt (T308) / GAPDH / pAkt (S473) / GAPDH

D. Glucose mg/dl/μg protein

Agpat2	+/+	+/+	+/+	+/+	-/-	-/-	-/-	-/-
Insulin	-	+	-	+	-	+	-	+
C18:1/20:4 PA	-	-	+	+	-	-	+	+

E. *G6pase* mRNA (fold change)

Agpat2	+/+	+/+	+/+	+/+	-/-	-/-	-/-	-/-
Insulin	-	+	-	+	-	+	-	+
C18:1/20:4 PA	-	-	+	+	-	-	+	+

F. *Pepck* mRNA (fold change)

Agpat2	+/+	+/+	+/+	+/+	-/-	-/-	-/-	-/-
Insulin	-	+	-	+	-	+	-	+
C18:1/20:4 PA	-	-	+	+	-	-	+	+

G. *G6pase* promoter activity (fold change)

Agpat2	+/+	+/+	+/+	+/+	+/+	-/-	-/-	-/-	-/-	-/-
pGL3B	+	-	-	-	-	+	-	-	-	-
G6pase	-	+	+	+	+	-	+	+	+	+
Insulin	-	-	+	-	+	-	-	+	-	+
C18:1/20:4 PA	-	-	-	+	+	-	-	-	+	+

H. *Pepck* promoter activity (fold change)
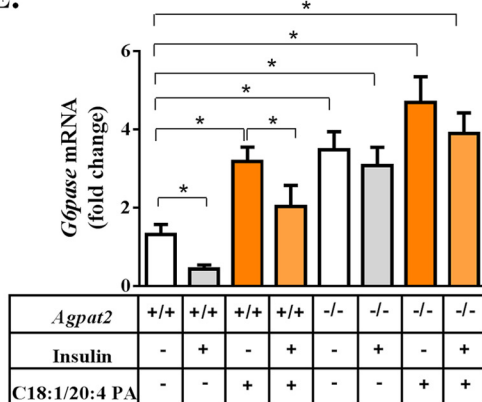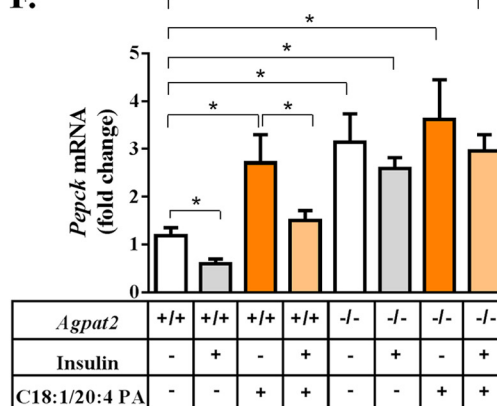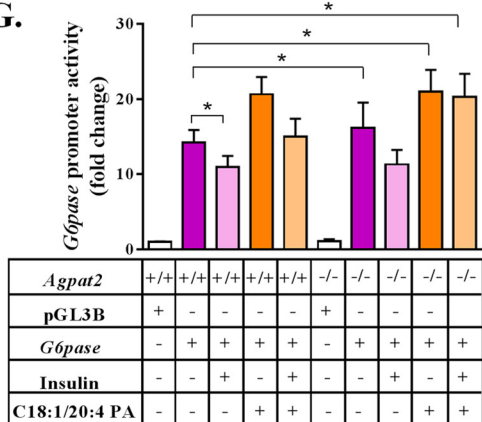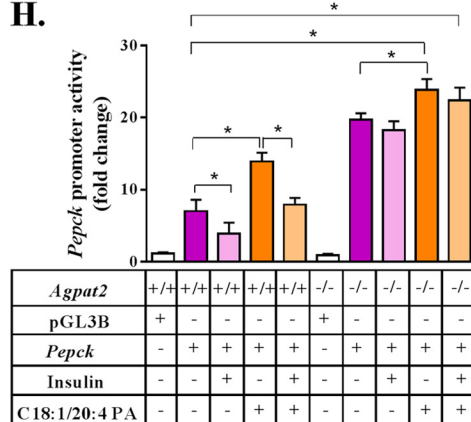
Agpat2	+/+	+/+	+/+	+/+	+/+	-/-	-/-	-/-	-/-	-/-
pGL3B	+	-	-	-	-	+	-	-	-	-
Pepck	-	+	+	+	+	-	+	+	+	+
Insulin	-	-	+	-	+	-	-	+	-	+
C18:1/20:4 PA	-	-	-	+	+	-	-	-	+	+

FIGURE 8. **Hepatic lipogenesis is independent of PA induction.** *A* and *B,* expression of mRNA for *Acc1* and *Fas* in primary hepatocytes from wild type (WT) and *Agpat2*$^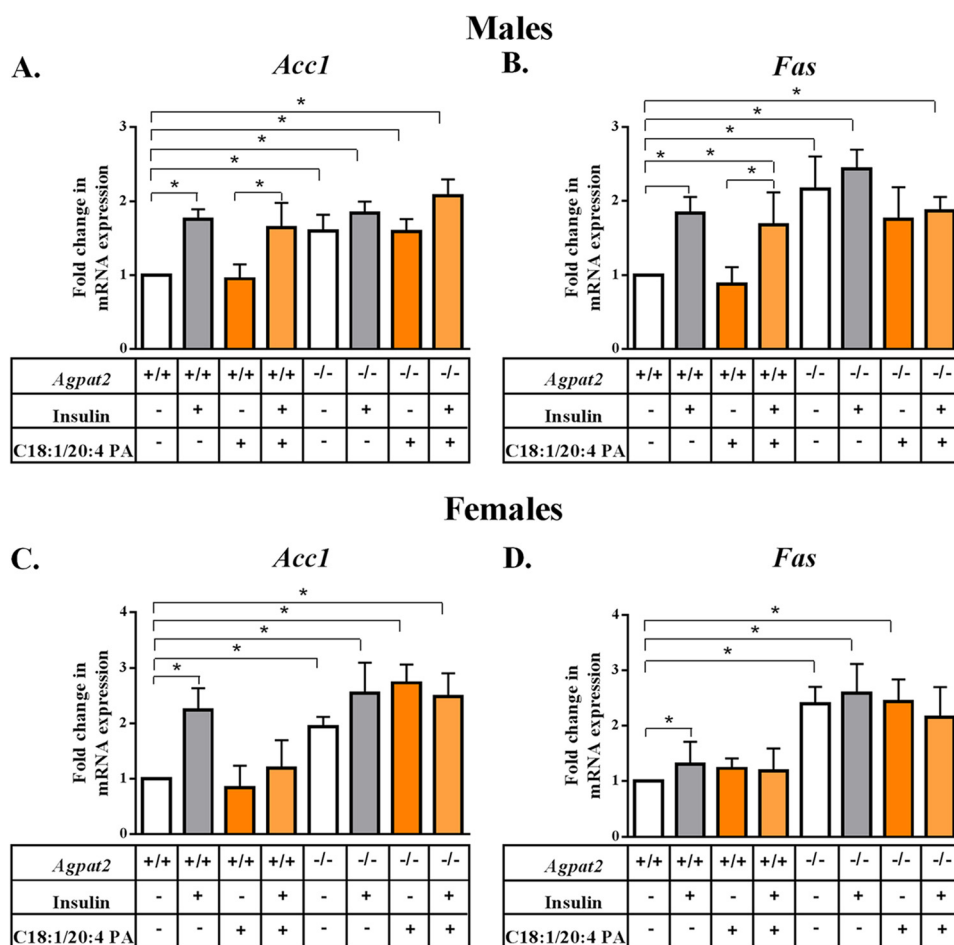{-/-}$ male mice. *Acc1* and *Fas* were analyzed by Q-PCR and normalized to cyclophilin. Shown are the fold-changes compared with untransfected WT primary mouse hepatocytes (expressed as mean ± S.E., $n = 4$). The expression of both *Acc1* and *Fas* remained unchanged in the presence of C18:1/20:4 PA. *C* and *D,* expression of mRNA for *Acc1* and *Fas* in hepatocytes isolated from WT and *Agpat2*$^{-/-}$ female mice. *Acc1* and *Fas* were analyzed similar to the male mice. The expression of both *Acc1* and *Fas* remained unchanged in the presence of C18:1/20:4 PA. The *p* values are shown *above* the bars (*, <0.05).

for key lipogenesis enzymes *Acc1* and *Fas* were measured (Fig. 8). We observed that in the presence of C18:1/20:4 PA, the mRNA levels of Acc1 and *Fas* remained unchanged in the hepatocytes from male (Fig. 8, *A* and *C*) and female (Fig. 8, *B* and *D*) WT and *Agpat2*$^{-/-}$ mice.

DISCUSSION

In this study we find that four PAs, C16:0/18:2, C16:0/18:1, C18:0/20:3, and C18:1/20:4, were significantly increased in the livers of *Agpat2*$^{-/-}$ mice. Among these only two PAs: C16:0/18:1 and C18:1/20:4 increased HGP in the mouse primary hepatocytes. The increase in HGP was accompanied by increased mRNA levels of the key gluconeogenic enzymes *G6pase* and *Pepck*. Luciferase reporter assays confirmed these PAs induced the transcription of the *G6pase* and *Pepck* genes. In *Agpat2*$^{-/-}$

hepatocytes, glucose production was also increased by PA, which was accompanied by increased mRNA expression of *G6pase* and *Pepck* and their respective luciferase reporter constructs. HGP was suppressed by insulin in WT but not *Agpat2*$^{-/-}$ hepatocytes.

Despite the near negligible AGPAT activity in the livers of *Agpat2*$^{-/-}$ mice, the levels of both the substrate (LPA) and the product (PA) remained elevated in mice of both genders. The high levels of PA may be due to additional source(s) like *Pld* and *Dagk*. It is unclear which pathway is important for the generation of PA in *Agpat2*$^{-/-}$ mice livers. Although the *Pld* expression was increased in these livers (*Pld*3 was increased ~2.2-fold in male livers and *Pld*4 was increased ~4-fold in female livers), we believe that the increased PA is most likely due to increased expression of *Dagk*3 (increased ~4- to ~9-fold) in livers of both

FIGURE 7. **Primary hepatocytes from *Agpat2*$^{-/-}$ female mice are insulin resistant.** *A* and *B,* quantification of LPA and PA in primary hepatocytes isolated from WT and *Agpat2*$^{-/-}$ female mice. The LPA and PA levels remained unchanged in *Agpat2*$^{-/-}$ hepatocytes when compared with WT hepatocytes, $n = 4$. *C,* immunoblot analysis of total Akt and its phosphorylated forms, pAkt-Thr-308 and pAkt-Ser-473. *D,* glucose output in primary hepatocytes isolated from *Agpat2*$^{-/-}$ female mice. C18:1/20:4 PA increased glucose output in primary hepatocytes and insulin was unable to suppress the gluconeogenesis, $n = 4$. *E* and *F,* expression of *G6pase* and *Pepck* was analyzed by Q-PCR and normalized to cyclophilin. The expression of both gluconeogenic genes was increased in the presence of PA. Insulin failed to suppress gluconeogenesis ($n = 4$). *G* and *H,* change in promoter activity of *G6pase* and *Pepck* as measured by the dual luciferase assay and expressed as fold-change compared with pGL3 basic in primary hepatocytes from *Agpat2*$^{-/-}$ female mice (expressed as mean ± S.E., $n = 4$). The *p* values are shown *above* the bars (*, <0.001; **, <0.01; †, <0.05).

Wild type   *Agpat2⁻/⁻*
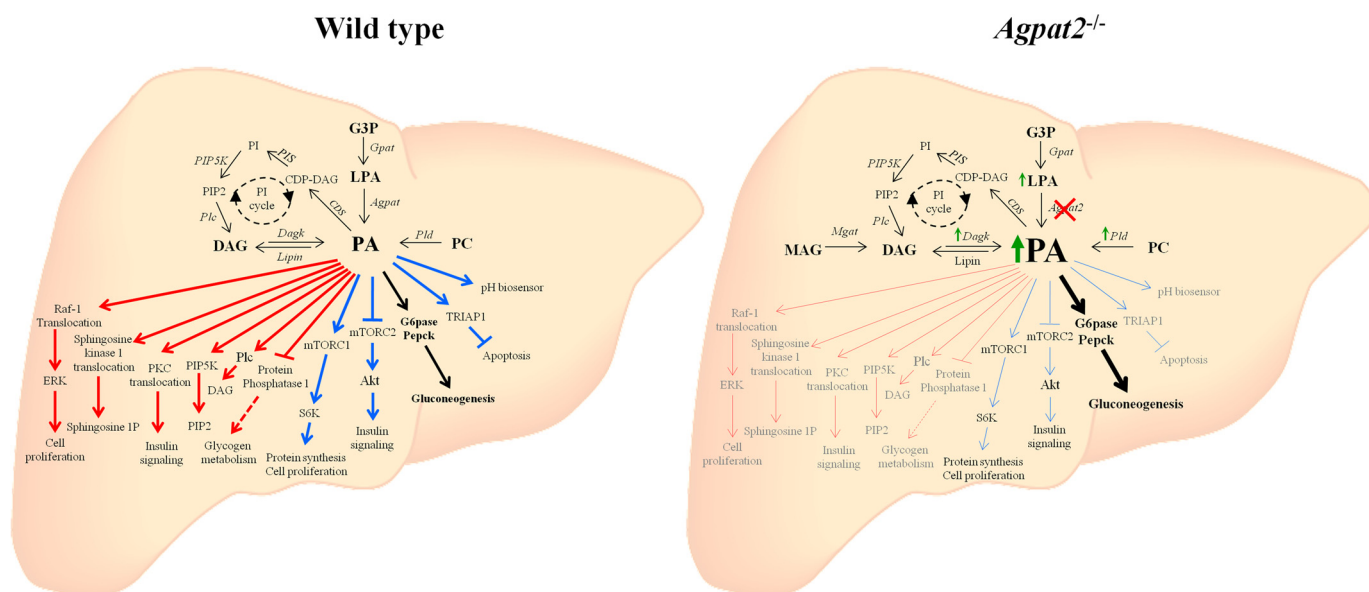
FIGURE 9. **Schematic of the various pathways, both known and speculative, leading to synthesis of PA and its function in liver.** PA can be formed in four different ways: 1) glycerol-3-phosphate (*G3P*) is acylated by glycerol-3-phosphate acyltransferase (*Gpat*) to form LPA with further acylation of LPA to PA by 1-acylglycerol-3-phosphate-O-acyltransferase (*Agpats*); 2) hydrolysis of phosphatidylcholine (PC) to PA by phospholipase D (PLD); 3) phosphorylation of DAG to PA by diacylglycerol kinase (*Dagk*); and 4) by the PI cycle. In PI cycle, PA is converted to cytidine diphosphate-diacylglycerol (*CDP-DAG*) an intermediate for the synthesis of PI in the presence of cytidine diphosphate-diacylglycerol synthase (*CDS*). CDP-DAG is converted to PI by PI synthase (*PIS*). The conversion of PI to PI-4,5-bisphosphate (*PIP₂*) is carried out by PI 4-phosphate 5-kinase (*PIP5K*). DAG can be formed by hydrolysis of PIP₂ by phospholipase C (*Plc*). This is a speculative PA synthesis cycle that awaits experimental confirmation. In certain pathological conditions as in the *Agpat2⁻/⁻* lipodystrophic mouse, DAG can be synthesized by acylation of monoacylglycerol (*MAG*) by monoacylglycerol acyltransferase (*MGAT1*) (7) or by de-phosphorylation of PA by lipin. *Mgat1* is not expressed in the livers of adult wild type mouse. PA is a lipid signaling molecule and modulates multiple pathways occurring at various subcellular sites in the cell. The role of PA at the membrane level is shown in *red arrows*, in the cytoplasm in *blue arrows*, and at the lysosomal level in *green arrows*. The most important and novel finding of our study is regulation of gluconeogenesis by PA, which is shown in *black arrows*. The role of PAs as a cellular pH sensor is shown in *pink*. These various pathways shown are compiled from the published literature. *Raf-1*, rapidly accelerated fibrosarcoma proto-oncogene serine/threonine-protein kinase (39); *ERK*, extracellular signal-regulated kinase; *PKC*, protein kinase C (40); *mTORC1*, mammalian target of rapamycin complex 1 (9); *S6K*, ribosomal protein S6 kinase; *mTORC2*, mammalian target of rapamycin complex 2 (35); *Akt*, protein kinase B; *G6pase*, glucose-6-phosphatase; *Pepck*, phosphoenolpyruvate carboxykinase (this study); *TRIAP1*, tumor protein p53 regulated inhibitor of apoptosis 1 (41); pH biosensor (42); sphingosine kinase (43); *PIP5K*, phosphatidylinositol 4-phosphate 5-kinase (44); *Plc*, phospholipase C (45); and *Pp1*, protein phosphatase 1 (26).

genders of *Agpat2⁻/⁻* mice. Furthermore, when AGPAT2 was overexpressed in livers of *Agpat2⁻/⁻* mice, it did not result in any improvement in hepatic steatosis or IR (12) suggesting that the elevated PAs are not products of the AGPAT2 enzyme. Further studies are required to determine which of these pathways is employed for the generation of PA.

How does PA affect IR in the livers of *Agpat2⁻/⁻* mice? In this study, we did not observe any novel PA species in the livers of *Agpat2⁻/⁻* mice. However, the levels of several PA species were increased. Based on the *m/z* ratio for LPA and PA and specific determination of the *sn-2* fatty acid released using PLA₂, we could determine the most probable PA species: C16:0/18:2, C16:0/18:1, and C18:1/20:4 PA. The most interesting observation of this study was that the addition of certain molecular species of PA increased gluconeogenesis in primary mouse hepatocytes and this increase was suppressed by insulin. We found that PA containing unsaturated fatty acids at both *sn-1* and *sn-2* positions (C18:1/20:4 PA) was very effective in increasing gluconeogenesis, whereas C16:0/18:2 PA was ineffective. Furthermore, C16:0/18:1 PA was as efficient as C18:1/20:4 PA in increasing gluconeogenesis. Previous studies have shown the preferred acyl-CoA for AGPAT2 in decreasing order as follows: C18:2 > C18:1 > C16:0 > C14:0 > C20:4-CoAs (12, 24). Thus C18:1/20:4 PA is less likely to be produced by AGPAT2 and more likely by the alternative pathways mentioned above.

The PA-induced glucose production appears to be due to the induction of key gluconeogenic genes *G6pase* and *Pepck*.

Although a few proteins such as mTOR, phosphatidylinositol 4-phosphate 5-kinase (PI4P5K), protein phosphatase (PP1Cγ), and protein kinase (PKCε) have been shown to interact with PA (25–27); the molecular and cellular mechanisms by which PA exerts its effects are still unknown. Recent experiments show that PA could also bind to the FK506-binding protein (FKBP12)-rapamycin-binding domain (11) and, in fact, some studies show that PA enhances mTOR activity (10). However, when primary mouse hepatocytes were incubated with specific PA species (C16:0/18:2, C16:0/18:1 and C18:1/20:4 PA), mTOR and its molecular targets remained unchanged. Identifying proteins that interact with PA could provide clues to the activation of *G6pase* and *Pepck*.

To examine the defective insulin signaling, we explored the PI3K-Akt pathway in whole livers of *Agpat2⁻/⁻* mice. Full activation of Akt requires phosphorylation at Thr-308 (28) by PDK1 and at Ser-473 in the C-terminal hydrophobic motif by mTORC2 (23). A recent study in obese type 2 diabetic *db/db* mice showed that knockdown of NADPH oxidase 4 resulted in sustained phosphorylation at Thr-308 but not at Ser-473, suggesting that the Thr-308 phosphorylation site is more insulin sensitive (29). We found that C16:0/18:1 PA and C18:1/20:4 PA decreased the phosphorylation of Akt at Thr-308, but not at Ser-473, which we interpret as inhibition of mTOR activity. Thus, this observation suggests that phosphorylation of Akt (pAkt-Thr-308) is PA specific. Overall, these *in vitro* studies in primary mouse hepatocytes revealed that specific PA species

could inhibit Akt phosphorylation at Thr-308 but failed to affect the phosphorylation at Ser-473.

The phosphorylation of Akt at Thr-308 by PDK1 was also significantly decreased in livers of $Agpat2^{-/-}$ mice. Normally PIP$_3$, the second messenger of PI3K, recruits Akt and PDK1 to the plasma membrane via their PH domains. The current study suggests that Akt or PDK1 or both fail to be recruited onto the plasma membrane and thus Akt is inefficiently phosphorylated (30). Prior studies have shown that when a mutation was created in the PH domain of PDK1 at serine 241 to alanine, it resulted in a 50-fold decrease in the phosphorylation and activation of Akt (31). It is also possible that PDK1 exists in its inactive state in livers of $Agpat2^{-/-}$ mice. The study reported by Seong *et al.* (32) showed that the apoptosis signal-regulating kinase 1 inhibits PDK1 function by phosphorylating PDK1 at Ser-394 and Ser-398. Furthermore, the same group reported that murine protein serine/threonine kinase 38 (*MPK38*) also interacts with PDK1 both *in vitro* and *in vivo* and inactivates it by phosphorylating at Thr-354 (33). This suggests that PDK1 activity may be inhibited by apoptosis signal-regulating kinase 1 or MPK38 resulting in decreased phosphorylation of Akt at Thr-308 in $Agpat2^{-/-}$ mice livers. Whether this pathway is altered by PA in AGPAT2 knockout livers will require further studies.

Two previous reports have attempted to demonstrate a role of PA in insulin signaling (34, 35). Zhang *et al.* (35) observed an increase in total LPA, PA, and DAG levels and also a modest increase in glucose output in primary mouse hepatocytes from WT mice overexpressing GPAT1. However, it is unclear if this is specifically due to PA, LPA, or DAG or a combination of these lipids (Fig. 1*E* in Ref. 35). These authors do show that only C16:0/16:0 PA was biologically active in inhibiting mTORC2 (Fig. 6*B* in Ref. 35). However, evidence supporting the role of C16:0/16:0 PA in glucose output was not provided. Of note, we did not detect the C16:0/16:0 PA species in our $Agpat2^{-/-}$ mouse model and although $Gpat1^{-/-}$ hepatocytes are protected from IR our $Agpat2^{-/-}$ hepatocytes are insulin resistant. A second important enzyme critical in PA metabolism is lipin, which dephosphorylates PA to DAG. All three lipin isoforms, lipin 1, lipin 2, and lipin 3, are known to be expressed in the liver (36). Ryu *et al.* (34) showed that overexpression of lipin 1 in WT hepatocytes leads to an increase in DAG levels (34). This did not regulate the phosphorylation of Akt, a key molecule for insulin signaling. However, the decrease in phosphorylation of Akt was only noted when the hepatocytes were incubated with PA, resulting in increased mRNA levels for *Pepck*, suggesting that PA could increase gluconeogenesis (Fig. 3*D* in Ref. 34). These two studies focused on the role of PA and its effect on Akt and mTOR pathways and insulin resistance. Our study now directly demonstrates the role of specific molecular species of PA in gluconeogenesis. However, the detailed molecular mechanism involved in PA-induced gluconeogenesis remains to be studied.

The current study provides an explanation for increased hepatic gluconeogenesis and IR present in livers of $Agpat2^{-/-}$ mice. As shown in insulin-sensitive WT hepatocytes, insulin suppresses gluconeogenesis despite the provision of exogenous PA to the hepatocytes. In contrast, in insulin-resistant $Agpat2^{-/-}$ hepatocytes where Akt could not be phosphorylated by PDK1, PA continues to stimulate glucose production. Further

studies are required to determine how and why PDK1 fails to activate Akt in these mice. Because PA is the substrate for the biosynthesis of phosphatidylinositol it could possibly generate a different molecular species of phosphatidylinositol whose configuration is such that it fails to recruit Akt and PDK1 to the plasma membrane. PA is also a signaling molecule and as shown in Fig. 9 is involved in several signaling pathways at all subcellular levels. This study now provides another layer of specificity for PA transduction as these pathway(s) might require specific molecular species of PAs.

This study might also have implications in understanding gluconeogenesis in cancer cells. Studies have implicated increased expression of AGPAT2 in the development of ovarian cancer (37), which should increase cellular PA levels. These observations would indicate that increased PA levels might increase gluconeogenesis more so in the insulin resistant state found in obesity and provide a role for PA as part of a pathway to supply energy to cancer cells (38).

REFERENCES

1. Agarwal, A. K., and Garg, A. (2003) Congenital generalized lipodystrophy. Significance of triglyceride biosynthetic pathways. *Trends Endocrinol. Metab.* **14,** 214–221
2. Coleman, R. A., and Lee, D. P. (2004) Enzymes of triacylglycerol synthesis and their regulation. *Prog Lipid Res.* **43,** 134–176
3. Agarwal, A. K. (2012) Lysophospholipid acyltransferases. 1-Acylglycerol-3-phosphate *O*-acyltransferases. From discovery to disease. *Curr. Opin Lipidol.* **23,** 290–302
4. Agarwal, A. K., Arioglu, E., De Almeida, S., Akkoc, N., Taylor, S. I., Bowcock, A. M., Barnes, R. I., and Garg, A. (2002) AGPAT2 is mutated in congenital generalized lipodystrophy linked to chromosome 9q34. *Nat. Genet.* **31,** 21–23
5. Vantyghem, M. C., Balavoine, A. S., Douillard, C., Defrance, F., Dieudonne, L., Mouton, F., Lemaire, C., Bertrand-Escouflaire, N., Bourdelle-Hego, M. F., Devemy, F., Evrard, A., Gheerbrand, D., Girardot, C., Gumuche, S., Hober, C., Topolinski, H., Lamblin, B., Mycinski, B., Ryndak, A., Karrouz, W., Duvivier, E., Merlen, E., Cortet, C., Weill, J., Lacroix, D., and Wemeau, J. L. (2012) How to diagnose a lipodystrophy syndrome. *Ann. Endocrinol.* **73,** 170–189
6. Garg, A. (2011) Clinical review. Lipodystrophies. Genetic and acquired body fat disorders. *J. Clin. Endocrinol. Metab.* **96,** 3313–3325
7. Cortés, V. A., Curtis, D. E., Sukumaran, S., Shao, X., Parameswara, V., Rashid, S., Smith, A. R., Ren, J., Esser, V., Hammer, R. E., Agarwal, A. K., Horton, J. D., and Garg, A. (2009) Molecular mechanisms of hepatic steatosis and insulin resistance in the AGPAT2-deficient mouse model of congenital generalized lipodystrophy. *Cell Metab.* **9,** 165–176
8. Gale, S. E., Frolov, A., Han, X., Bickel, P. E., Cao, L., Bowcock, A., Schaffer, J. E., and Ory, D. S. (2006) A regulatory role for 1-acylglycerol-3-phosphate-*O*-acyltransferase 2 in adipocyte differentiation. *J. Biol. Chem.* **281,**

11082–11089

9. Toschi, A., Lee, E., Xu, L., Garcia, A., Gadir, N., and Foster, D. A. (2009) Regulation of mTORC1 and mTORC2 complex assembly by phosphatidic acid. Competition with rapamycin. *Mol. Cell. Biol.* **29,** 1411–1420

10. Yoon, M. S., Sun, Y., Arauz, E., Jiang, Y., and Chen, J. (2011) Phosphatidic acid activates mammalian target of rapamycin complex 1 (mTORC1) kinase by displacing FK506-binding protein 38 (FKBP38) and exerting an allosteric effect. *J. Biol. Chem.* **286,** 29568–29574

11. Rodriguez Camargo, D. C., Link, N. M., and Dames, S. A. (2012) The FKBP-rapamycin binding domain of human TOR undergoes strong conformational changes in the presence of membrane mimetics with and without the regulator phosphatidic acid. *Biochemistry* **51,** 4909–4921

12. Agarwal, A. K., Sukumaran, S., Cortés, V. A., Tunison, K., Mizrachi, D., Sankella, S., Gerard, R. D., Horton, J. D., and Garg, A. (2011) Human 1-acylglycerol-3-phosphate O-acyltransferase isoforms 1 and 2. Biochemical characterization and inability to rescue hepatic steatosis in *Agpat2*$^{-/-}$ gene lipodystrophic mice. *J. Biol. Chem.* **286,** 37676–37691

13. Baker, D. L., Desiderio, D. M., Miller, D. D., Tolley, B., and Tigyi, G. J. (2001) Direct quantitative analysis of lysophosphatidic acid molecular species by stable isotope dilution electrospray ionization liquid chromatography-mass spectrometry. *Anal. Biochem.* **292,** 287–295

14. Becart, J. C., Biesse, J.P. (1990) Quantitative analysis of phospholipids by HPLC with a light scattering evaporating detector. Application to raw materials for cosmetic use. *J. High Resolution Chromatogr.* **13,** 126–129

15. Lepage, G., Roy, C. C. (1986) Direct transesterification of all classes of lipids in a one-step reaction. *J. Lipid Res.* **27,** 114–120

16. Devaiah, S. P., Roth, M. R., Baughman, E., Li, M., Tamura, P., Jeannotte, R., Welti, R., and Wang, X. (2006) Quantitative profiling of polar glycerolipid species from organs of wild-type *Arabidopsis* and a phospholipase Dα1 knockout mutant. *Phytochemistry* **67,** 1907–1924

17. Welti, R., Li, W., Li, M., Sang, Y., Biesiada, H., Zhou, H. E., Rajashekar, C. B., Williams, T. D., and Wang, X. (2002) Profiling membrane lipids in plant stress responses. Role of phospholipase Dα in freezing-induced lipid changes in Arabidopsis. *J. Biol. Chem.* **277,** 31994–32002

18. Arneson, L. S., Kunz, J., Anderson, R. A., and Traub, L. M. (1999) Coupled inositide phosphorylation and phospholipase D activation initiates clathrin-coat assembly on lysosomes. *J. Biol. Chem.* **274,** 17794–17805

19. Martelli, A. M., Tabellini, G., Bortul, R., Manzoli, L., Bareggi, R., Baldini, G., Grill, V., Zweyer, M., Narducci, P., and Cocco, L. (2000) Enhanced nuclear diacylglycerol kinase activity in response to a mitogenic stimulation of quiescent Swiss 3T3 cells with insulin-like growth factor I. *Cancer Res.* **60,** 815–821

20. Shimomura, I., Bashmakov, Y., Ikemoto, S., Horton, J. D., Brown, M. S., and Goldstein, J. L. (1999) Insulin selectively increases SREBP-1c mRNA in the livers of rats with streptozotocin-induced diabetes. *Proc. Natl. Acad. Sci. U.S.A.* **96,** 13656–13661

21. Matsuda, M., Korn, B. S., Hammer, R. E., Moon, Y. A., Komuro, R., Horton, J. D., Goldstein, J. L., Brown, M. S., and Shimomura, I. (2001) SREBP cleavage-activating protein (SCAP) is required for increased lipid synthesis in liver induced by cholesterol deprivation and insulin elevation. *Genes Dev.* **15,** 1206–1216

22. Alessi, D. R., Deak, M., Casamayor, A., Caudwell, F. B., Morrice, N., Norman, D. G., Gaffney, P., Reese, C. B., MacDougall, C. N., Harbison, D., Ashworth, A., and Bownes, M. (1997) 3-Phosphoinositide-dependent protein kinase-1 (PDK1). Structural and functional homology with the *Drosophila* DSTPK61 kinase. *Curr. Biol.* **7,** 776–789

23. Sarbassov, D. D., Guertin, D. A., Ali, S. M., and Sabatini, D. M. (2005) Phosphorylation and regulation of Akt/PKB by the rictor-mTOR complex. *Science* **307,** 1098–1101

24. Hollenback, D., Bonham, L., Law, L., Rossnagle, E., Romero, L., Carew, H., Tompkins, C. K., Leung, D. W., Singer, J. W., and White, T. (2006) Substrate specificity of lysophosphatidic acid acyltransferase β. Evidence from membrane and whole cell assays. *J. Lipid Res.* **47,** 593–604

25. Fang, Y., Vilella-Bach, M., Bachmann, R., Flanigan, A., and Chen, J. (2001) Phosphatidic acid-mediated mitogenic activation of mTOR signaling. *Science* **294,** 1942–1945

26. Jones, J. A., Rawles, R., and Hannun, Y. A. (2005) Identification of a novel phosphatidic acid binding domain in protein phosphatase-1. *Biochemistry* **44,** 13235–13245

27. Stace, C. L., and Ktistakis, N. T. (2006) Phosphatidic acid- and phosphatidylserine-binding proteins. *Biochim. Biophys. Acta* **1761,** 913–926

28. Alessi, D. R. (2001) Discovery of PDK1, one of the missing links in insulin signal transduction. Colworth Medal Lecture. *Biochem. Soc. Trans.* **29,** 1–14

29. Wu, X., and Williams, K. J. (2012) NOX4 pathway as a source of selective insulin resistance and responsiveness. *Arterioscler. Thromb. Vasc. Biol.* **32,** 1236–1245

30. Bayascas, J. R., Wullschleger, S., Sakamoto, K., García-Martínez, J. M., Clacher, C., Komander, D., van Aalten, D. M., Boini, K. M., Lang, F., Lipina, C., Logie, L., Sutherland, C., Chudek, J. A., van Diepen, J. A., Voshol, P. J., Lucocq, J. M., and Alessi, D. R. (2008) Mutation of the PDK1 PH domain inhibits protein kinase B/Akt, leading to small size and insulin resistance. *Mol. Cell. Biol.* **28,** 3258–3272

31. Casamayor, A., Morrice, N. A., and Alessi, D. R. (1999) Phosphorylation of Ser-241 is essential for the activity of 3-phosphoinositide-dependent protein kinase-1. Identification of five sites of phosphorylation *in vivo*. *Biochem. J.* **342,** 287–292

32. Seong, H. A., Jung, H., Ichijo, H., and Ha, H. (2010) Reciprocal negative regulation of PDK1 and ASK1 signaling by direct interaction and phosphorylation. *J. Biol. Chem.* **285,** 2397–2414

33. Seong, H. A., Jung, H., Manoharan, R., and Ha, H. (2012) PDK1 protein phosphorylation at Thr-354 by murine protein serine-threonine kinase 38 contributes to negative regulation of PDK1 protein activity. *J. Biol. Chem.* **287,** 20811–20822

34. Ryu, D., Oh, K. J., Jo, H. Y., Hedrick, S., Kim, Y. N., Hwang, Y. J., Park, T. S., Han, J. S., Choi, C. S., Montminy, M., and Koo, S. H. (2009) TORC2 regulates hepatic insulin signaling via a mammalian phosphatidic acid phosphatase, LIPIN1. *Cell Metab.* **9,** 240–251

35. Zhang, C., Wendel, A. A., Keogh, M. R., Harris, T. E., Chen, J., and Coleman, R. A. (2012) Glycerolipid signals alter mTOR complex 2 (mTORC2) to diminish insulin signaling. *Proc. Natl. Acad. Sci. U.S.A.* **109,** 1667–1672

36. Donkor, J., Sariahmetoglu, M., Dewald, J., Brindley, D. N., and Reue, K. (2007) Three mammalian lipins act as phosphatidate phosphatases with distinct tissue expression patterns. *J. Biol. Chem.* **282,** 3450–3457

37. Springett, G. M., Bonham, L., Hummer, A., Linkov, I., Misra, D., Ma, C., Pezzoni, G., Di Giovine, S., Singer, J., Kawasaki, H., Spriggs, D., Soslow, R., and Dupont, J. (2005) Lysophosphatidic acid acyltransferase-β is a prognostic marker and therapeutic target in gynecologic malignancies. *Cancer Res.* **65,** 9415–9425

38. Finley, L. W., Zhang, J., Ye, J., Ward, P. S., and Thompson, C. B. (2013) SnapShot. Cancer metabolism pathways. *Cell Metab.* **17,** 466–466.e2

39. Rizzo, M. A., Shome, K., Watkins, S. C., and Romero, G. (2000) The recruitment of Raf-1 to membranes is mediated by direct interaction with phosphatidic acid and is independent of association with Ras. *J. Biol. Chem.* **275,** 23911–23918

40. Limatola, C., Schaap, D., Moolenaar, W. H., and van Blitterswijk, W. J. (1994) Phosphatidic acid activation of protein kinase C-ζ overexpressed in COS cells. Comparison with other protein kinase C isotypes and other acidic lipids. *Biochem. J.* **304,** 1001–1008

41. Potting, C., Tatsuta, T., König, T., Haag, M., Wai, T., Aaltonen, M. J., and Langer, T. (2013) TRIAP1/PRELI complexes prevent apoptosis by mediating intramitochondrial transport of phosphatidic acid. *Cell Metab.* **18,** 287–295

42. Shin, J. J., and Loewen, C. J. (2011) Putting the pH into phosphatidic acid signaling. *BMC Biol.* **9,** 85

43. Delon, C., Manifava, M., Wood, E., Thompson, D., Krugmann, S., Pyne, S., and Ktistakis, N. T. (2004) Sphingosine kinase 1 is an intracellular effector of phosphatidic acid. *J. Biol. Chem.* **279,** 44763–44774

44. Moritz, A., De Graan, P. N., Gispen, W. H., and Wirtz, K. W. (1992) Phosphatidic acid is a specific activator of phosphatidylinositol-4-phosphate kinase. *J. Biol. Chem.* **267,** 7207–7210

45. Henry, R. A., Boyce, S. Y., Kurz, T., and Wolf, R. A. (1995) Stimulation and binding of myocardial phospholipase C by phosphatidic acid. *Am. J. Physiol.* **269,** C349–358